SANDIA REPORT

SAND90—3134 • UC—721
Unlimited Release
Printed July 1991

In Situ Measurements of Rock Salt Permeability Changes Due to Nearby Excavation

J. C. Stormont, C. L. Howard, J. J. K. Daemen

Prepared by
Sandia National Laboratories
Albuquerque, New Mexico 87185 and Livermore, California 94550
for the United States Department of Energy
under Contract DE-AC04-76DP00789

Issued by Sandia National Laboratories, operated for the United States Department of Energy by Sandia Corporation.

Available to DOE and DOE contractors from
Office of Scientific and Technical Information
PO Box 62
Oak Ridge, TN 37831

Prices available from (615) 576-8401, FTS 626-8401

Available to the public from
National Technical Information Service
US Department of Commerce
5285 Port Royal Rd
Springfield, VA 22161

NTIS price codes
Printed copy: A05
Microfiche copy: A01

SAND--90-3134

DE92 002215

SAND90-3134
Unlimited Release
July 1991

In Situ Measurements of Rock Salt Permeability Changes Due to Nearby Excavation

J. C. Stormont
Repository Isolation Systems Division
Sandia National Laboratories
Albuquerque, NM 87185

C. L. Howard
RE/SPEC, Inc.
Carlsbad, NM 88220

J. J. K. Daemen
Mackay School of Mines
University of Nevada
Reno, NV 89557

Abstract

The Small-Scale Mine-By was an in situ experiment to measure changes in brine and gas permeability of rock salt as a result of nearby excavation. A series of small-volume pressurized brine- and gas-filled test intervals were established 8 m beneath the floor of Room L1 in the WIPP underground. The test intervals were isolated in the bottom of the 4.8-cm diameter monitoring boreholes with inflatable rubber packers, and are initially pressurized to about 2 MPa. Both brine- and gas-filled test intervals were located 1.25, 1.5, 2, 3, and 4 r from the center of a planned large-diameter hole, where r is the radius of the large-diameter hole. Prior to the drilling of the large diameter borehole, the responses of both the brine- and gas-filled test intervals were consistent with the formation modeled as a very low permeability, low porosity porous medium with a significant pore (brine) pressure and no measurable gas permeability. The drilling of the mine-by borehole created a zone of dilated, partially saturated rock out to about 1.5 r. The formation pressure increases from near zero at 1.5 r to the pre-excavation value at 4 r. Injection tests reveal a gradient of brine permeabilities from 5×10^{-18} m^2 at 1.25 r to about the pre-excavation value (10^{-21} m^2) by 3 r. Gas-injection tests reveal measurable gas permeability is limited to within 1.5 r.

Contents

Figures

Tables

1 Introduction

A Disturbed Rock Zone (DRZ) develops around the excavations of the Waste Isolation Pilot Plant (WIPP), a US Department of Energy research and development facility in bedded salt (halite) near Carlsbad, New Mexico. The DRZ is defined as the zone of rock in which mechanical and hydrologic properties have changed in response to excavation (Borns and Stormont, 1988). The presence of a DRZ has numerous implications for the performance of the WIPP. The DRZ is relatively permeable compared to the undisturbed formation, and must be considered in seal systems designed to isolate waste. The increased porosity of the DRZ may also serve as a sink for fluids (brine or gas) to accumulate. Most research has focused on the properties and response of the rock mass outside the DRZ. Current mechanical and hydrologic models for rock salt do not account for the observed behavior in the DRZ.

Hydrologic characterization of the formation at the storage horizon has principally been accomplished with brine pressure build-up and injection tests. These borehole tests are performed in isolated intervals usually deep enough into the formation so that they are assumed to be outside the DRZ. These data have been reasonably well matched with conventional models of transient flow in a porous medium. The data from the various measurements indicate that the storage horizon halite has a permeability of less than 10^{-20} m^2 and a pore pressure up to 13 MPa (Peterson et al., 1987; Nowak and McTigue, 1987; Saulnier and Avis, 1988; Nowak et al., 1988; Beauheim et al., 1991; Howarth et al., 1991). The porosity is typically assumed to be on the order of 0.1 and 1.0%.

Numerous gas-injection tests were made from isolated intervals within single boreholes to delineate the DRZ. In the test intervals which were comprised solely of rock salt and were within the first meter from an excavation, the interpreted permeabilities varied from about 10^{-13} to 10^{-19} m^2. The interpreted gas permeabilities rapidly decrease with distance from an excavation so that by 2 to 5 meters from an excavation the gas permeability of the rock salt is immeasurably small. Undisturbed brine-saturated rock salt has a very small or perhaps non-existent gas permeability because in order to flow, gas must overcome both the formation (brine) pressure as well as a threshold capillary pressure which has been estimated to be in excess of 10 MPa (Stormont et al., 1987). Measurable gas flow in the DRZ may be through flow paths created subsequent to excavation. This additional porosity might include brine-saturated pores of sufficient size that their capillary pressures are very low, permitting gas flow. It is more likely that the flow paths for gas are not completely brine-saturated, and the gas flows through the available gas-filled pore volume. From previous gas flow measurements (Stormont et al., 1987; Stormont, 1990a), we conclude that the DRZ is principally a dilated, probably partially saturated zone which extends a limited distance from an excavation. Dilation and de-saturation of the rock salt surrounding WIPP excavations

have also been inferred from resistivity measurements (Borns and Stormont, 1988), seismic tomography (Borns and Stormont, 1988) and ultrasonic velocity and attenuation (Holcomb, 1988).

The purpose of the Small-Scale Mine-By Experiment is to monitor the hydrologic response of a halite layer to nearby excavation and provide a hydrologic measure of the DRZ. An array of small volume pressurized brine- and gas-filled test intervals located about 8 m from an underground room was first established. Their pressure response was monitored prior to, during and after the drilling (excavation or mine-by) of a nearby large-diameter hole. Sometime later, gas and brine-injection tests were conducted in the boreholes. The emphasis of measurements and analyses was to quantify the changes in gas and brine permeability as a result of excavation. The data also provide qualitative information regarding changes in dilation and saturation in response to excavation.

This report is organized as follows. Chapter 2 contains the experimental configurations and methods used to conduct this experiment. In Chapter 3, the analysis approach and scope is given. The experimental results and their interpretation are given in Chapter 4. In Chapter 5, the results are discussed. A summary of the experiment is given in Chapter 6, and is followed by a list of references. Appendix A provides a development of the analysis method.

2 Experimental Configuration and Methods

Twelve small-diameter "monitoring" boreholes were drilled vertically down from the floor of Room L1[1] in the experimental portion of the WIPP facility. The 4.8-cm diameter boreholes were drilled to a depth of 8 m with air as the drilling fluid. Test intervals were created in the bottom of the borehole by placing an inflatable rubber packer nominally 65 cm from the bottom of the borehole. A schematic diagram of the monitoring boreholes is given in Figure 1. In order to minimize the volume of test interval, a 4.3-cm diameter steel rod was placed near the bottom of the borehole. The packers have a tubing feed-through to allow access to the test interval for fluid injection or withdrawal. The test interval pressure is measured by means of a strain-gaged diaphragm pressure gage. A nearby data acquisition shed provides the excitation, signal conditioning, and data recording instrumentation.

Prior to initiating the tests, system tests were performed on all packer assemblies. During a system test, the packer assembly is placed in an aluminum tube, the packers are inflated and the test interval is pressurized and monitored to detect leaks. These tests revealed that all of the system components were operative with no detectable leaks. Because the small amount of flow observed along the packer-tubing interface was attributed to scratches in the tubing, leakage at the packer-borehole interface was not expected.

A plan view of the monitoring boreholes is given in Figure 2. As shown in Figure 2, both brine- and gas-filled monitoring boreholes were placed at 1.25, 1.5, 2, 3, and 4 r from the center of the planned large-diameter hole, where r is the radius of the large-diameter hole (r = 48.3 cm). Two monitoring boreholes of each type (gas and brine) were located at 1.25 r to provide redundancy at the location where the greatest changes in response to excavation were anticipated. At a depth of about 8 m from the floor of Room L1, the rock adjacent to the test interval is described as clear to moderately reddish orange halite with some polyhalite stringers and very little disseminated clay (USDOE, 1988). The nearest anhydrite or distinct clay seam is more than 2 m from the test intervals.

Both the brine- and gas-filled test intervals were established within 4 days of completion of the borehole drilling by placing the steel rod and packer at the desired location and inflating the packer. The packers were inflated and mainitained at a pressure of about 5 MPa using fresh water. For the brine-monitoring boreholes, saturated brine was first placed in the bottom of the borehole prior to placement of the packer and steel bar to reduce the likelihood of trapping gas in the test interval. The packers were driven at a pressure of about 5 MPa with fresh water. The brine and gas test intervals were pressurized to about 2 MPa, shut-in and monitored for about 150 days until the

[1]Room L1 is 9.9-m wide, 3.9-m high, and 30-m long, and was excavated in April, 1984. The boreholes for this experiment were drilled in October and November of 1988.

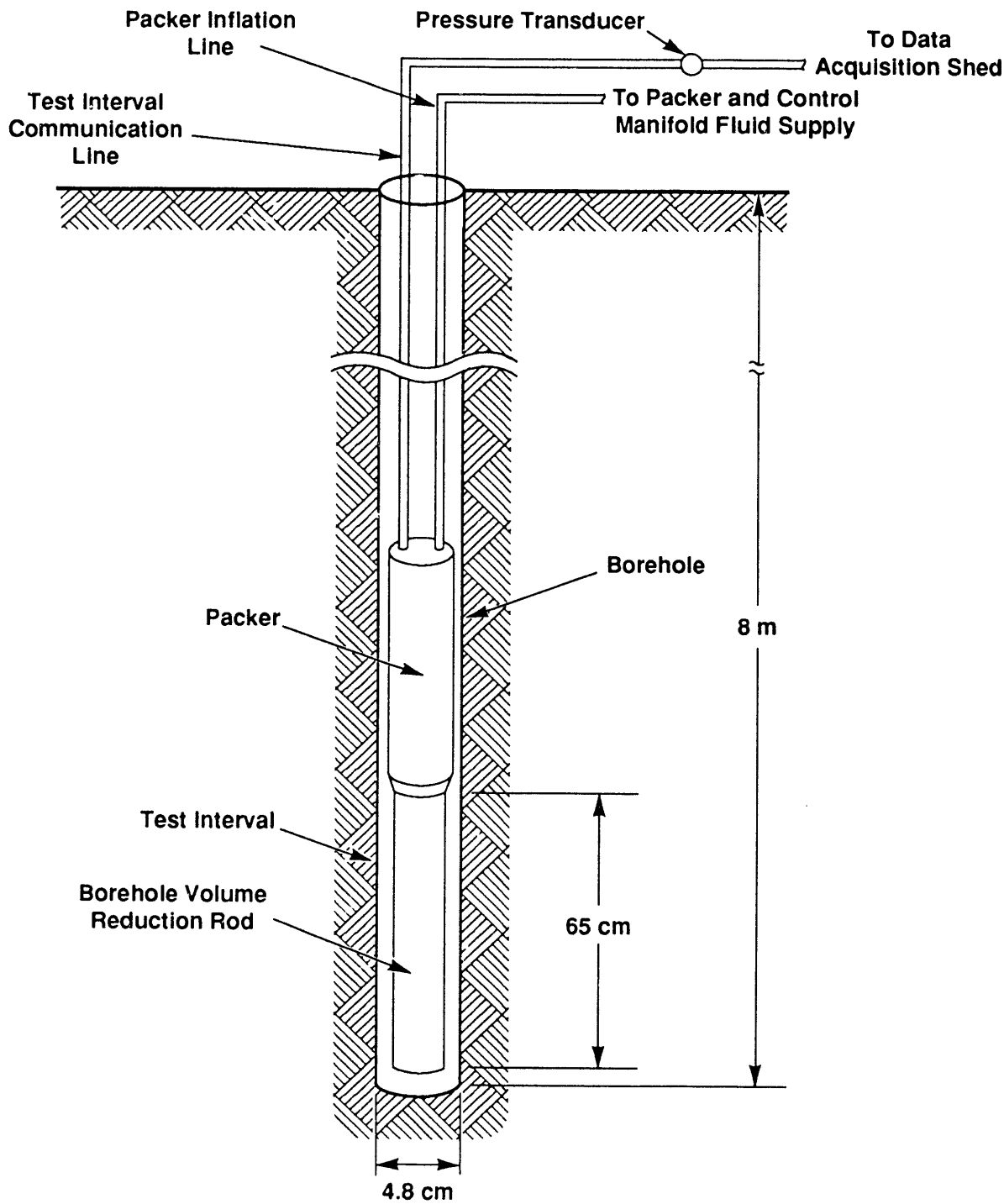

Figure 1: Schematic of monitoring borehole configuration.

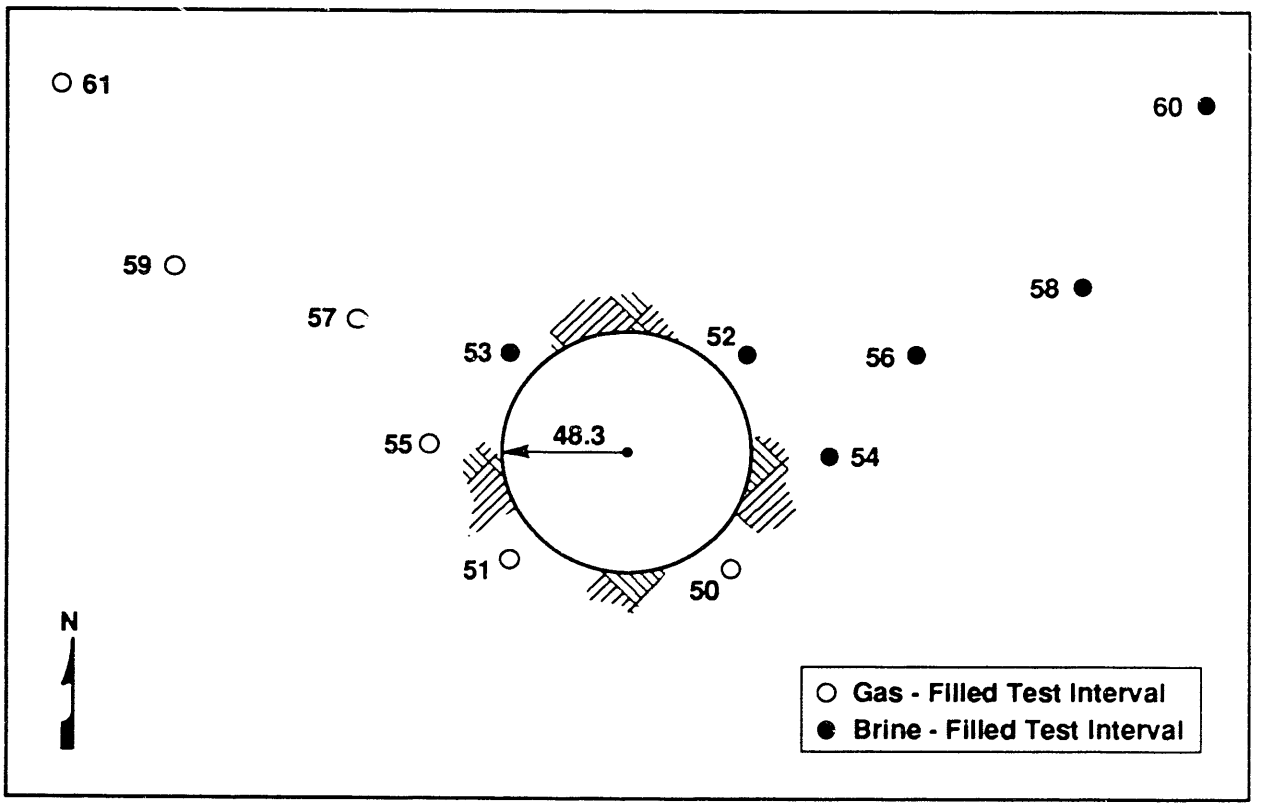

TRI-6346-90-0

Figure 2: Plan view of mine-by borehole (48.3-cm radius) and monitoring boreholes (4.8-cm diameter) on the floor of Room L1.

large-diameter hole was drilled. Time zero is taken as the time the first test interval was established. In one brine-filled test interval at 1.25 r, the borehole fluid and rock temperatures were measured with thermocouples.

Approximately 40 days after the first test interval was established, test interval compressibility measurements were made in the brine-filled test intervals. Two methods were used. In the first method, called the equilibration method, the test interval is allowed to equilibrate with a small reservoir of brine at a pressure less than that of the test interval. To compute the test interval compressibility, it is necessary to know the reservoir compressibility. The second method, called the vent method, involves venting a small volume of brine from the test interval into a buret at atmospheric pressure. In both methods, the pressure change in the test interval resulting from the flow of brine out of the test interval is measured.

Pulse tests were conducted in two test intervals. The pressure in one gas-filled test interval and one brine-filled test interval were instantaneously increased by about 1 MPa and 1.5 MPa, respectively, 140 days after the test intervals were established.

The mine-by was achieved by drilling a 96.5-cm diameter hole. This hole was deepened incrementally: A 5-cm diameter pilot hole was first drilled, followed by the coring of the 96.5-cm diameter hole to a similar depth. The pilot hole provided directional stability and aided in the large core removal. The drilling time was less than 8 hours for both the pilot hole and the large-diameter core from about 1 meter above to 1 meter below the mean test interval depth (8 m). To reduce the potential for packer-induced damage, packers within 2 r of the large-diameter borehole were shut-in prior to the mine-by so that their pressure would drop if they began to expand the borehole.

Approximately 50 days after the mine-by drilling, compressibility measurements were repeated in the brine-filled test intervals using the equilibration method. Also, the gas volumes in the gas-filled test intervals were measured by permitting them to equilibrate with a small reservoir at a known pressure.

About 240 days after the mine-by drilling, injection tests were conducted in both the brine-filled and gas-filled test intervals. Constant-pressure tests were conducted in all of the brine-filled test intervals and two of the gas-filled test intervals. the test interval pressures were increased by up to 0.7 MPa, and the flow rate necessary to maintain this pressure was measured with a flow manifold connected at the wellhead. Shut-in or pressure-decay test were performed in three gas-filled test intervals by raising the pressure in the test interval by 1.4 MPa and measuring the pressure decrease as fluid flows out into the formation.

At the conclusion of the testing, the position of the packer system in the borehole was verified. For those holes in which the packer systems could be removed, the hole diameter was measured with a caliper.

3 Analysis Approach and Scope

The principal focus of the data analysis from the in situ experiment is to determine the changes in permeability of the rock salt as a result of nearby excavation. The analysis approach is to first establish a pre-excavation permeability and then determine the permeability after the excavation. Analyses of the experimental data are in three categories:

(1) Pre-excavation response: Prior to excavation of the large-diameter borehole (mine-by), the responses of the brine- and gas-filled test intervals can be interpreted to provide baseline or initial formation properties.

(2) Excavation-induced response: During and after the mine-by, the responses of the test intervals can be interpreted in terms of the changing formation properties.

(3) Post-excavation injection tests: Approximately 240 days after the mine-by, the pressures in the test intervals were at or near equilibrium values. At this time, injection tests were conducted in all of the gas- and brine-filled test intervals. These tests provide data which can be interpreted in terms of formation properties.

The experimental data are interpreted in terms of transient flow through a compressible, porous medium. The flow is assumed to be radial, applicable for flow to or from a borehole. The governing differential equation for isothermal, radial flow through a porous medium is derived by combining the continuity equation, the equation of state of the fluid, and Darcy's law. For brine flow it is given as

$$\frac{\partial P}{\partial t} = \frac{1}{S}\frac{1}{r}\frac{\partial}{\partial r}\left(\frac{k}{\mu} r \frac{\partial P}{\partial r}\right) \tag{1}$$

where P is the borehole pressure, t is time, r is the radial coordinate, μ is the fluid viscosity, and k is the permeability. S is a formation storage term given as

$$S = (C - C_s) + \phi(C_f - C_s) \tag{2}$$

where C is the bulk compressibility of the rock, C_s is the compressibility of the solids, C_f is the compressibility of the fluids, and ϕ is the porosity. An expression comparable to Equation 1 can be developed for gas flow with P replaced by P^2 and substitution of the appropriate gas properties.

There are five boundary conditions applicable at the test interval: (1) brine flow to or from a brine-filled, shut-in test interval, (2) brine flow to or from a partially gas-filled, shut-in test interval, (3) pressure-pulse gas injection, (4) constant-pressure brine injection, and (5) constant-pressure gas injection. Closure of the test interval from salt creep can be accounted for in each of these cases. Derivations of the equations for brine and gas flow as well as applicable boundary conditions are given in Appendix A. A finite difference solution to Equation 1 was developed in order to simulate the field measurements of brine and gas flow. Details of the numerical solution are given in Appendix A.

The lower limit of the meaurement system resolution depends on the uncertainties and limitations of the test system and interpretation method. The measured quantities during these flow tests are pressure, test region dimensions (e.g., test interval length), test interval compressibility, and time. With the exception of brine-filled test interval compressibility, these quantities are measured quite accurately. For all the gas tests and the constant-pressure brine-injection tests, the uncertainity in the measured quantities is expected to contribute a maximum of 10% relative error to the calculated flow rates and permeabilities. For the brine-filled test interval pressure build-up tests, the uncertainity in the brine-filled test interval compressibility results in relative error in the flow rate and permeability of about 100%. Further discussion of this topic can be found in Stormont et al. (1987) and Stormont (1990a).

The greatest potential uncertainty in the calculated permeabilities, however, is a result of the flow model itself. The development of the governing differential equation (Appendix A) is accompanied by numerous conventional assumptions. Some of the assumptions are readily justified (e.g., isothermal conditions). Other assumptions are more difficult to justify (e.g., a single-phase fluid is flowing; permeability is independent of fluid pressure; the flow is perfectly radial). However, in the absence of more information, these assumptions are necessary in order to make the model tractable. Further discussion of some of these assumptions is given in Appendix A.

4 Results

4.1 Pre-excavation responses

The responses of the brine- and gas-filled test intervals after they were shut-in but before excavation of the mine-by borehole are given in Figures 3 and 4, respectively. Once shut-in, the brine-filled test interval pressures increase and approach a value of about 3 MPa. Borehole 60 appears to be appraching a somewhat greater value. The gas-filled test interval pressures increase at slower but more linear rates. The responses of the gas-filled test intervals appear to be more variable than those of the brine-filled test intervals.

The response of both the brine- and gas-filled test intervals are consistent with the formation modeled as a porous medium with a very low permeability, low porosity, and a significant pore (brine) pressure. Flow of brine from the formation into the lower pressure test intervals results in pressure increases in both the brine- and gas-filled test intervals. The flow rates into the test intervals, and consequently the test interval pressure changes, decrease as the test interval pressures approach the formation pore pressure, and finally level off near the formation pore pressure. In the gas-filled test intervals, pressures increase at slower rates due to the relatively great test interval compressibilities. The gas in the test intervals does not flow into the formation because (1) the formation brine is at a higher pressure, and (2) there is a threshold or displacement pressure which the gas would have to overcome in order to flow into the formation.

The formation properties are estimated by means of numerical simulations of the test. Permeability, porosity, formation pore pressure, test interval dimensions (including closure or opening of the test interval during the test), test interval compressibility, formation compressibility, and fluid properties are input to the simulation, and the resulting calculated pressure history is compared to the data. The values of the parameters which were fixed in the simulations - formation compressibilities, fluid properties, and test interval dimensions - are tabulated in Appendix A. The unknown parameters (permeability, porosity, and formation pressure) are adjusted until a reasonable agreement between the numerical simulation and measured response is obtained.

The numerical solution is non-unique: different combinations of parameters (permeability, porosity, and formation pressure) produce simulations which match the measured pressure histories. In order to eliminate one variable in the interpretation of the pre-excavation data, the formation porosity was assumed to be 0.1% for most of the calculations. This value is consistent with that used in previous analyses (Peterson et al., 1987; Stormont et al., 1987; Nowak et al., 1988; Howarth et al., 1991) and is within the range for healed or intact rock salt determined by Stormont (1990b). With this value of porosity, the formation storage term S computed by means of Equation 2 is

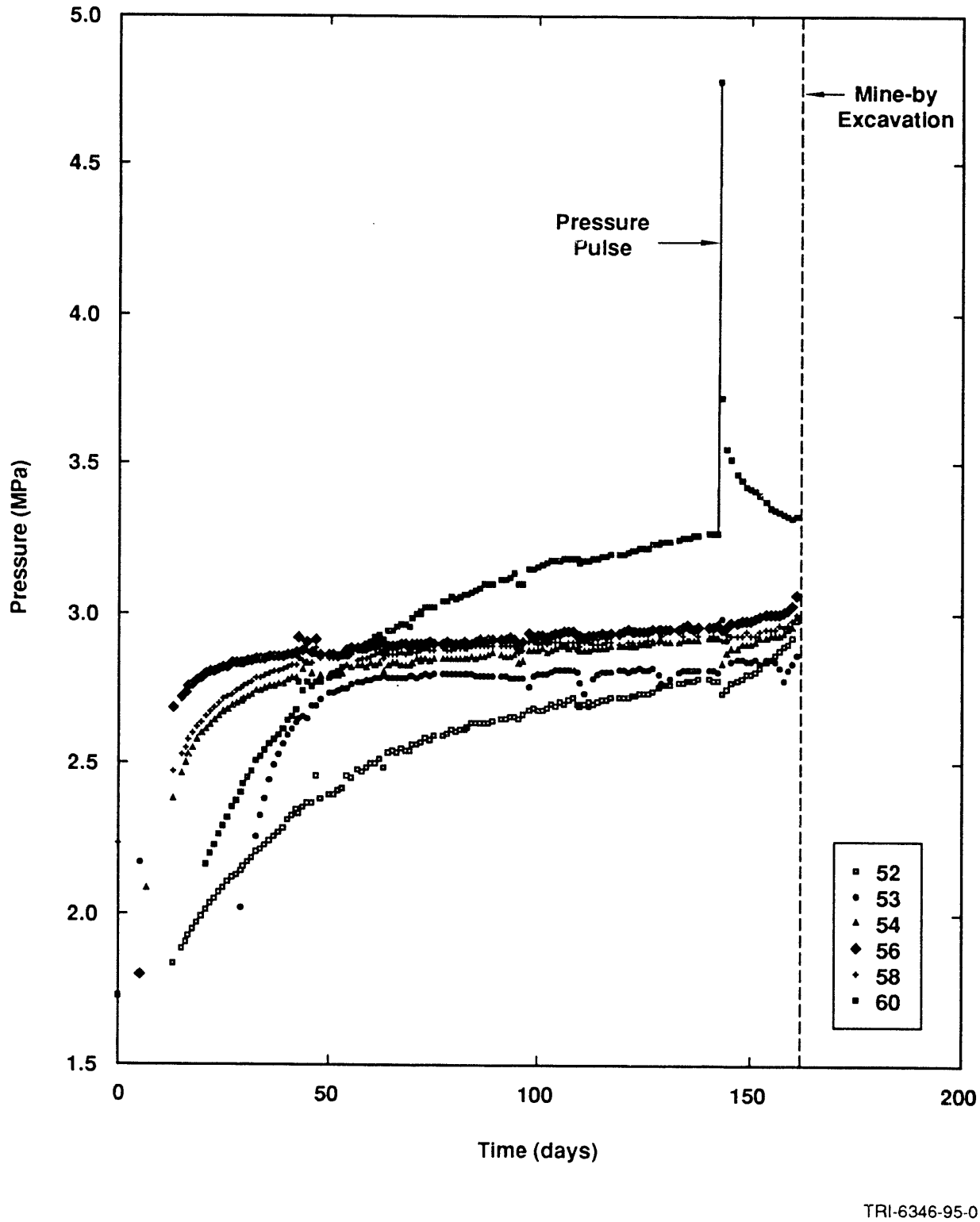

Figure 3: Pressure-time data from brine-filled test intervals prior to excavation.

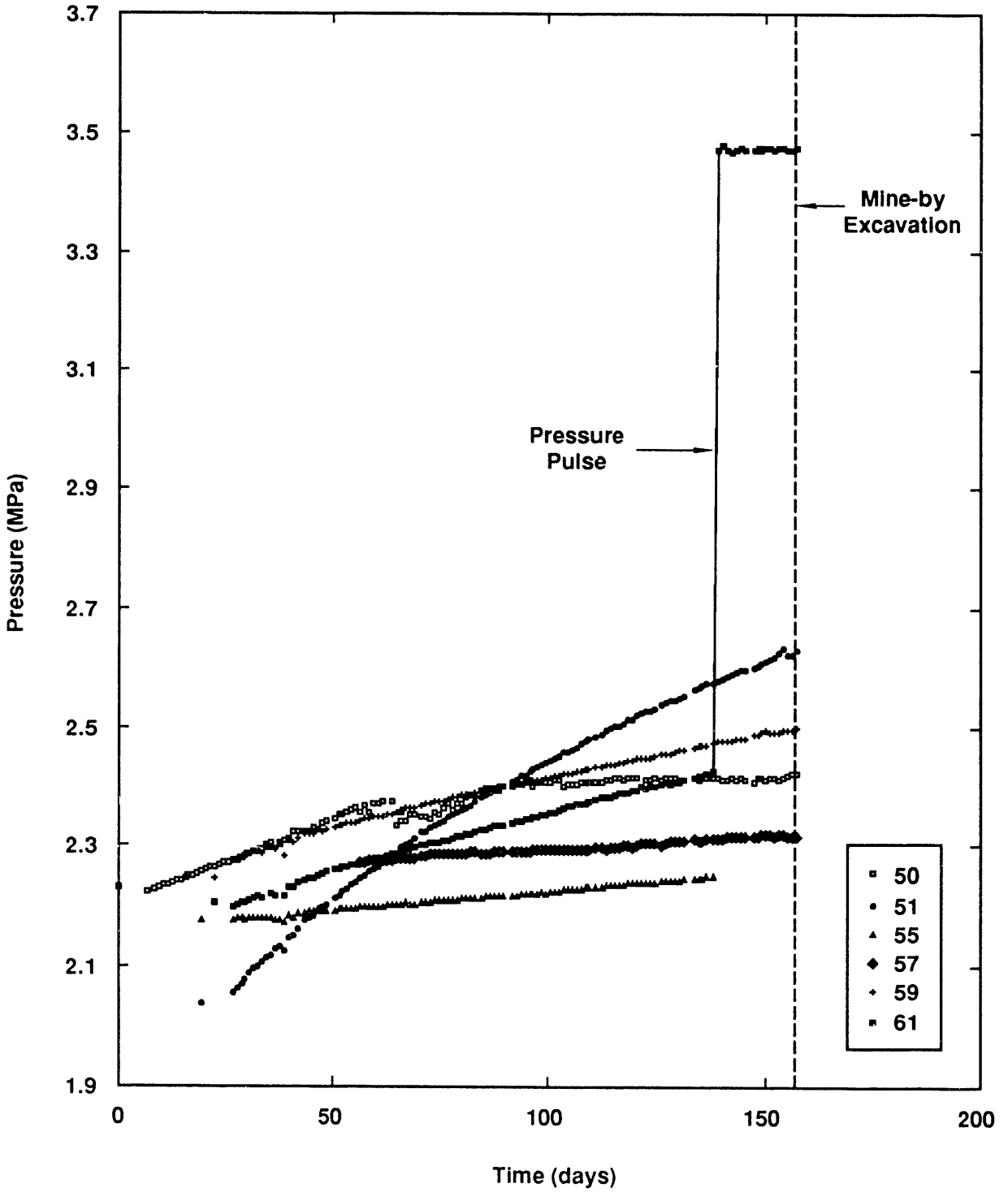

Figure 4: Pressure-time data from gas-filled test intervals prior to excavation. Data from borehole 55 are truncated due to data acquisition problem.

equivalent to that used for other simulations of brine flow in WIPP rock salt (Nowak et al., 1988; Howarth et al., 1991).

Another required input for the numerical simulations is the test interval compressibility. The test interval compressibility of the brine-filled test intervals can be dramatically different than the compressibility of brine alone. The presence of even small amounts of gas in the test interval will dominate the effective test interval compressibility. For example, at a test interval pressure of 2 MPa, 1% gas by volume will increase the test interval compressibility by an order of magnitude. For the brine-filled test intervals, gas could be trapped during packer installation or in the tubing, or could flow into the test interval from the formation or exsolve from formation brine in response to pressure decreases. Compliance of the packer system may also greatly affect the brine-filled test interval compressibility. The measurements of the test interval compressibility with the equilibration method resulted in calculated compressibilities less than that of brine itself. This non-physical result was subsequently explained by small gas bubbles trapped in the reservoir observed during an inspection of the measurement system. Test interval compressiblities determined from the vent method, given in Table I, are in the expected range (i.e., more than that for brine alone, about $3\text{x}10^{-10} Pa^{-1}$).

Table I: Brine-filled test interval compressibilities measured with vent method

Borehole number	Compressibility (Pa^{-1})
52	$2.7\text{x}10^{-9}$
53	$2.0\text{x}10^{-9}$
54	$1.6\text{x}10^{-9}$
60	$1.6\text{x}10^{-9}$

The approach to estimating the formation properties from the pre-excavation brine pressure responses was as follows. First, two groups of responses were defined. Group 1 (test intervals 52 and 60) had a test intervals (Group 2: test intervals 53, 54, 56 and 58). Next, simulations were conducted that produced subjective estimates of upper and lower bounds to the two groups of measured responses. The free variables in these simulations were permeability and formation pressure. Two values of test interval compressibilty that bounded the measured test interval compressibilities were used (Table I). All other variables were fixed (porosity, test zone dimensions, initial pressure, fluid properties). The brine data can be bounded with a formation pressure of 2.8 MPa to 3.5 MPa and a permeability of $1.7\text{x}10^{-22}$ to $5.6\text{x}10^{-21}$ m^2. The results of the numerical simulations that bound the measured responses are given in Figures 5 and 6 and summarized in Table II.

Simulations performed with a porosity of 1% rather than 0.1% altered the calculated pressures by less than 2% at any time, revealing the insignificance of the porosity to the

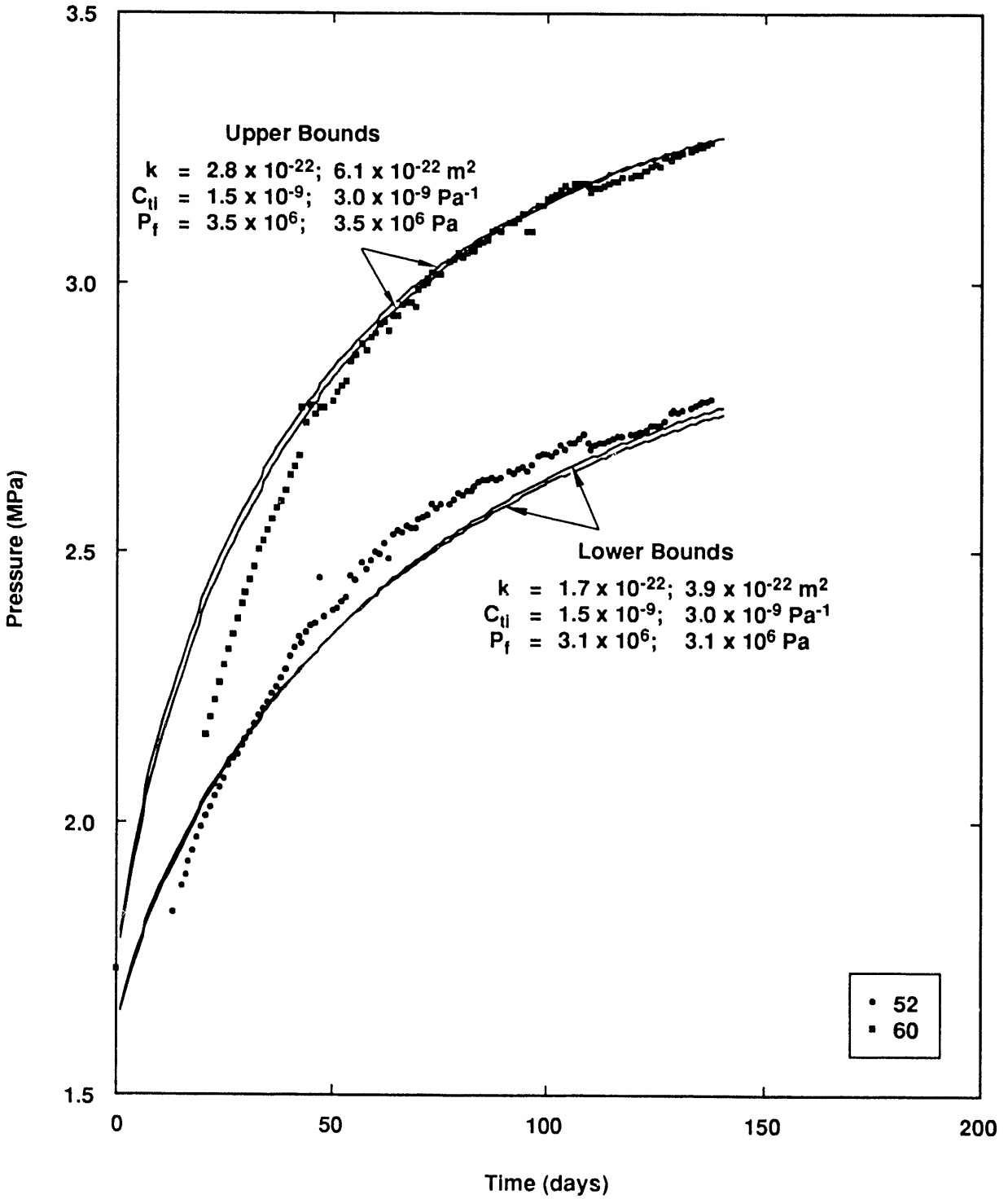

Figure 5: Bounding numerical simulations for Group 1 brine-filled test interval build-up data.

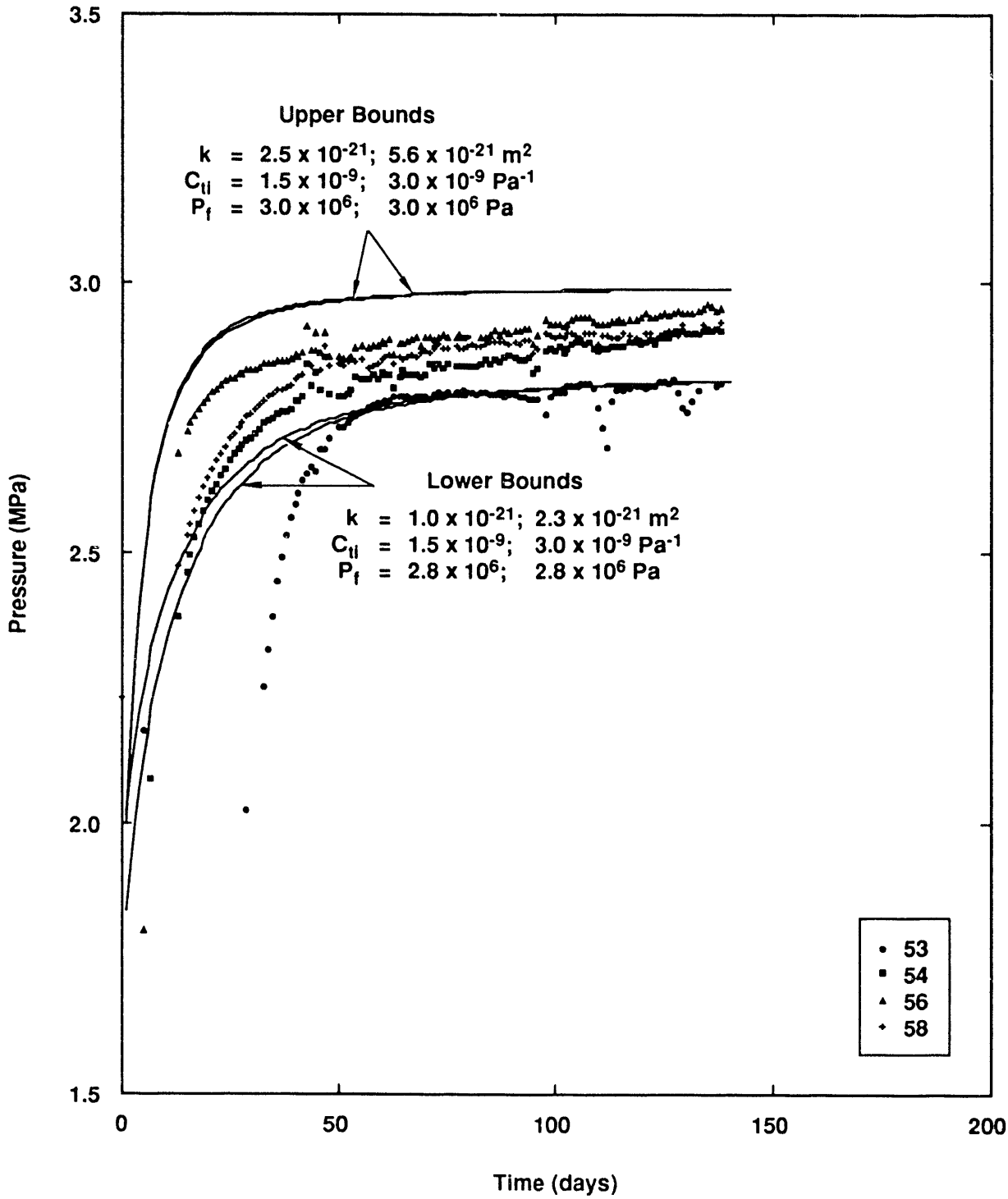

Figure 6: Bounding numerical simulations for Group 2 brine-filled test interval build-up data.

Table II: Results of Bounding Simulations of Pre-Excavation Brine-Filled Test Interval Responses

Group	Permeability (m^2)	Compressibility (Pa^{-1})	Formation pressure (Pa)
UPPER BOUNDS			
1	2.8×10^{-22}	1.5×10^{-9}	3.5×10^{6}
	6.1×10^{-22}	3.0×10^{-9}	3.5×10^{6}
2	2.5×10^{-21}	1.5×10^{-9}	3.0×10^{6}
	5.6×10^{-21}	3.0×10^{-9}	3.0×10^{6}
LOWER BOUNDS			
1	1.7×10^{-22}	1.5×10^{-9}	3.1×10^{6}
	3.9×10^{-22}	3.0×10^{-9}	3.1×10^{6}
2	1.0×10^{-21}	1.5×10^{-9}	2.8×10^{6}
	2.3×10^{-21}	3.0×10^{-9}	2.8×10^{6}

calculated response for these tests. A similar conclusion was reached for brine flow in WIPP rock salt by Howarth et al. (1991). This result is a consequence of the calculated response not being greatly affected by the formation storage S, the term in which the porosity manifests itself.

The responses of the gas-filled test intervals can also be grouped into two categories. Group 1 (test intervals 51, 59, and 61) had steeper pressure build-ups compared to Group 2 (test intervals 50, 55, and 57). As with the brine-filled test interval simulations, the approach was to find the combinations of permeabilities and formation pressures that bounded the two groups of measured responses. Because the compressibility of a gas-filled test interval is dominated by the compressibility of the gas, the test interval compressibility was not varied for these simulations. Both the measured data and the numerical simulations produced nearly linear pressure-time responses. It is the slope of the pressure history which the simulations bound; the calculated response was found to be relatively insensitive to the value of the assumed initial test interval pressure.

Simulations that bounded the gas-filled test interval responses are given in Figures 7 and 8 and are summarized in Table III. It was found that a formation pressure of 3.0 to 3.6 MPa and a permeability of 2.0×10^{-20} to 5.0×10^{-22} m^2 produced simulations which bounded these data. The interpreted permeabilities and formation pressures which bound the responses of the gas-filled test intervals prior to the mine-by are of the same magnitude as those determined from the brine-filled test interval responses. The range of interpreted permeabilities from the gas-filled test intervals is somewhat

Table III: Results of Bounding Simulations of of Pre-Excavation Gas-Filled Test Interval Responses

Group	Permeability (m^2)	Formation pressure (Pa)
UPPER BOUNDS		
1	$2.0x10^{-20}$	$3.6x10^6$
2	$5.0x10^{-21}$	$3.0x10^6$
LOWER BOUNDS		
1	$8.0x10^{-21}$	$3.6x10^6$
2	$5.0x10^{-22}$	$3.0x10^6$

greater than those from the brine-filled test intervals.

The magnitude of the formation pore pressure interpreted from the pressure build-ups (about 3 MPa) is less than the pore pressure of up to 13 MPa for the undisturbed formation estimated by others (e.g., Howarth et al., 1991). This indicates that the test intervals were located close enough to Room L1 (8 m) to be in a region of depressed pore pressure, or this halite layer had an anomalously low pore pressure.

140 days after the first test interval was shut-in, the pressure in the monitoring boreholes 61 (gas-filled) and 60 (brine-filled) were instantaneously increased (pulsed). In the gas-filled test interval, the pressure was increased from 2.4 to 3.5 MPa (see Figure 10). Even at this pressure, which is in the range of the local formation pressure, the gas pressure continued to increase, although more slowly, indicating that gas still could not flow from the test interval into the formation.

In contrast, when the pressure was instantaneously increased from 3.3 to 4.8 MPa in borehole 60 (brine-filled test interval), the pressure decreased and approached the pre-pulse pressure after a few days (see Figure 3). This result indicates flow of brine into the formation. However, the interpreted permeability from this pulse test is about two orders of magnitude greater than from the build-up data. Possible causes for the discrepancy include:

- Test interval compliance: a pulse of pressure could displace the packer, resulting in a decrease in pressure.
- Unaccounted for mechanical-hydrological coupling: the increase in pore pressure around the borehole may reduce the effective stress on the rock and the pore structure may dilate, locally increasing its permeability.
- A local, borehole-scale DRZ may exist: for the build-up test, the inflow to the

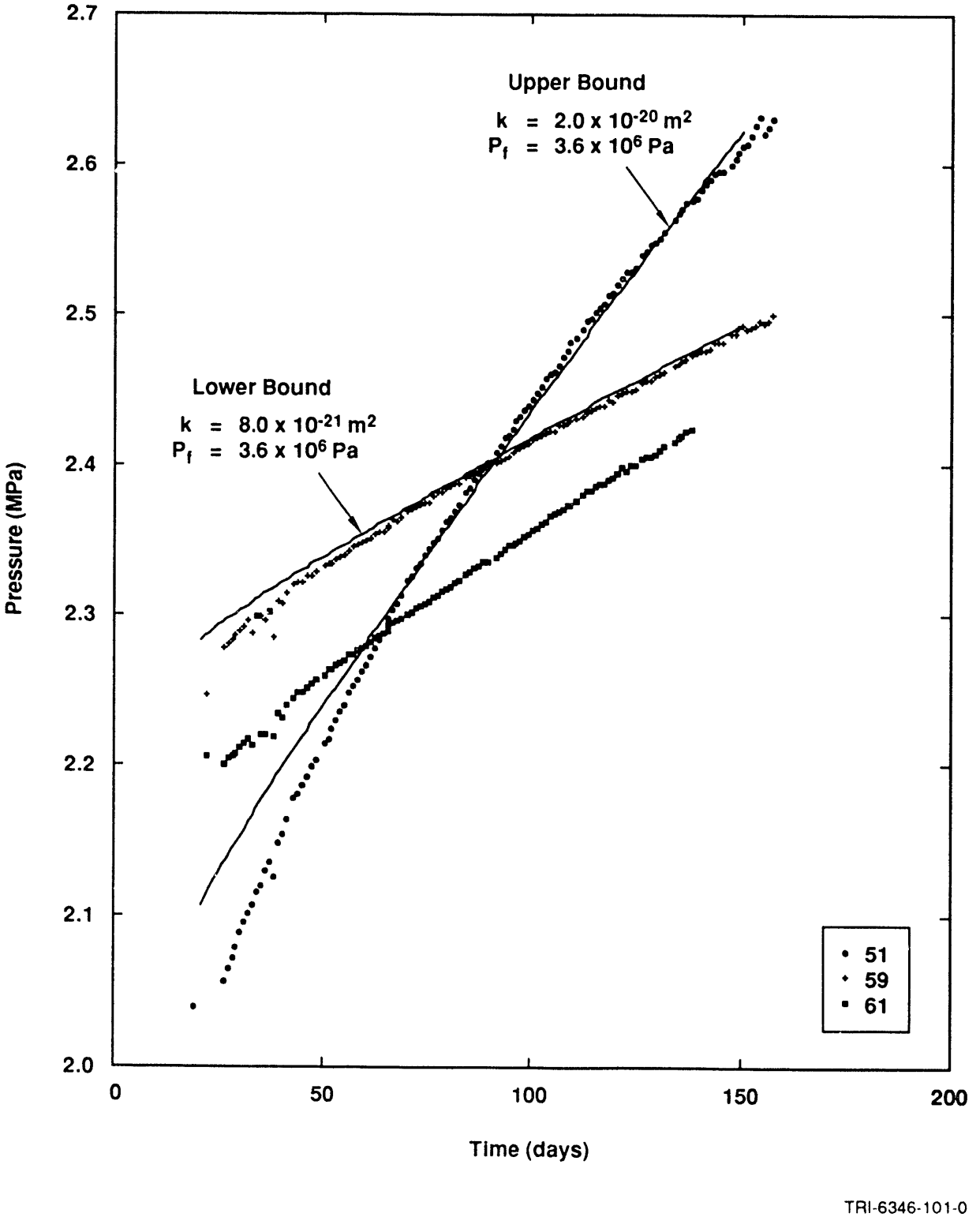

Figure 7: Bounding numerical simulations for Group 1 gas-filled test interval build-up data.

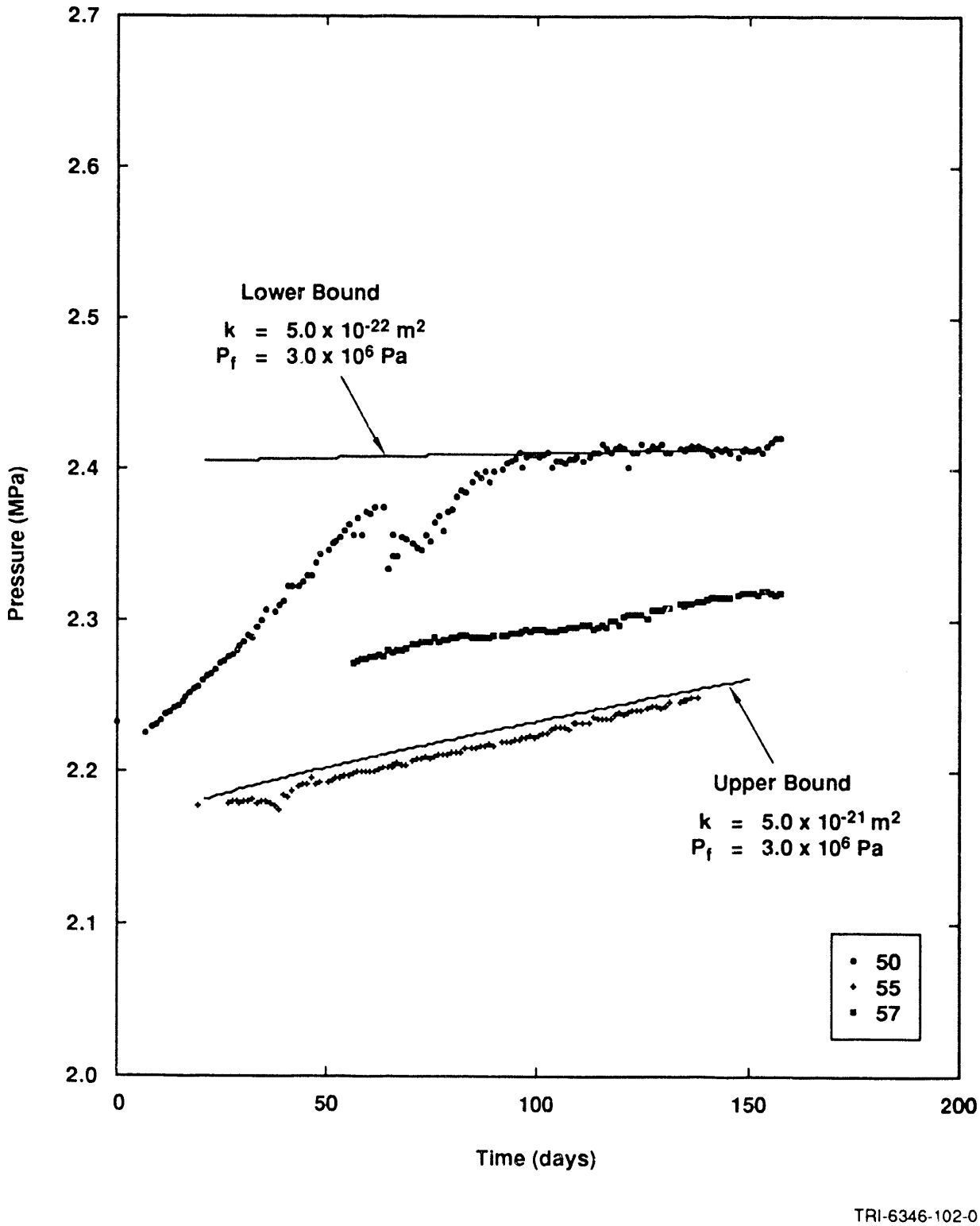

Figure 8: Bounding numerical simulations for Group 2 gas-filled test interval build-up data.

borehole is controlled by the far-field properties whereas for an injection test, the outflow is initially controlled by the near-field (local DRZ) properties.

Because the build-up data are believed to produce permeabilities more representative of the formation, we discounted the permeability interpreted from the pulse test in borehole 60.

The time-dependent creep of rock salt may change the volume of the monitoring boreholes, which in turn will induce pressure changes in test intervals that have been shut-in. When closure comparable to that measured in nearby open boreholes is included in the numerical simulations, the permeability could be reduced by about 10% or the formation pressure could be reduced by about 10% to match the data equally well compared to simulations with no closure. Thus, the assumed closure of the monitoring boreholes does not appear to dominate the fluid-pressure response of the test intervals. However, it is not clear how the borehole actually responds to salt creep and internal fluid pressure. Recent careful meaurements of borehole diameter changes in pressurized test intervals indicate that some holes open and some close (Howarth et al., 1991), suggesting a complex mechanical-hydrologic interaction.

In summary, the interpreted brine permeabilities are in the range expected for undisturbed rock salt. Further, the pre-excavation response shows that gas does not flow from the test intervals out into the formation. This indicates that the effective gas permeability of the formation prior to the mine-by excavation is zero.

4.2 Responses during and after excavation

The responses of the brine- and gas-filled test intervals during and after excavation are given in Figures 9 and 10, respectively. The brine-filled test interval responses reveal pressure increases during the excavation process followed by a period of decreasing pressures tending toward equilibrium values. The response of the brine-filled test intervals are a function of the distance of the test interval from the excavation; the closer to the excavation, the greater the initial increase, the more the pressure subsequently drops, and the lower the equilibrium pressure. At 1.25 and 1.5 r, the brine-filled test intervals lose nearly all of their pressure in response to excavation. From 1.5 r to 4 r, there is a gradient of increasing pressure. At 4 r, the pressure initially decreases after the mine-by but recovers to near the pre-excavation value.

During excavation, the pressures increase slightly in the gas-filled test intervals. The subsequent pressure decreases are a function of the distance a test interval is from the mine-by excavation. At 1.25 r and 1.5 r, the gas pressures drop rapidly to 0 and 0.7 MPa, respectively. At 2 r, the gas pressure changes from slowly increasing prior to the

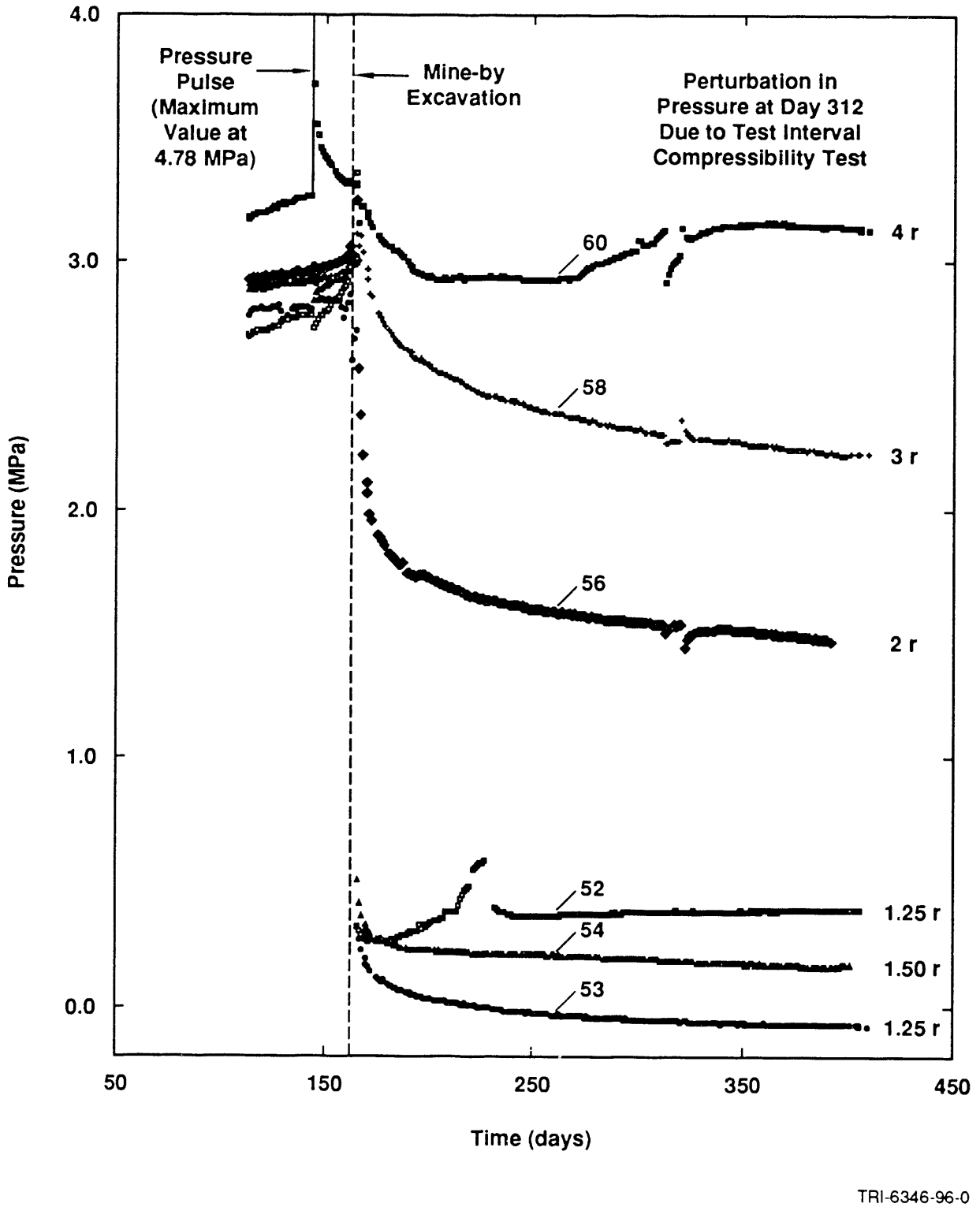

Figure 9: Pressure-time data from brine-filled test intervals during and following excavation.

mine-by to slowly decreasing afterward. At 3 and 4 r, there is no apparent response to excavation.

The peak pressures concurrent with excavation normalized with respect to the pre-excavation pressures are given in Figure 11. The peak pressures occurred within 15 minutes of one another in all test intervals, and coincided with the drilling of the large-diameter hole past the depth of the test intervals. One cause of the initial pressure increase is thermal expansion of the fluid in the test interval from heat generated by the drilling process. At the time the drilling passed by the test interval depth, the brine temperature at 1.25 r was measured as increasing by about 5 $^{\circ}C$. Assuming a volumetric thermal expansivity of $3\text{x}10^{-4}K^{-1}$ and a compressibility of $2\text{x}10^{-9}Pa^{-1}$ for the test interval brine, the measured temperature rise corresponds to a pressure increase of about 0.8 MPa, consistent with the measured pressure increases at this location. A similar temperature increase in the gas-filled test interval at 1.25 r would increase the pressure by about 35 kPa, similar to the measured pressure increases at 1.25 r. Lack of additional temperature measurements precludes conclusively ascribing the pressure increases in all of the test intervals to temperature effects.

Another possible cause of the pressure increase is stress changes induced by the excavation. Removal of the borehole material induces a stress wave that moves through the formation at a velocity of $> 10^3$ m/sec (see Carter and Booker, 1990, for further discussion). The resulting stress change could then cause (1) test interval closure, and (2) an elevated formation pore pressure. The test interval closures required to produce the measured pressure increases are consistent with an instantaneous elastic response, both in magnitude and its rapid decrease away from the excavation. A formation pore pressure increase is predicted from poroelastic theory (Nowak and McTigue, 1987). A portion of the mean stress change due to the excavation is instantaneously borne by the fluid phase, causing the fluid pressure to increase. This effect, however, is expected to cause a uniform pressure increase, whereas the data reveal a gradient away from the borehole.

The subsequent pressure decreases in the brine- and gas-filled test intervals are due to (1) dilation of the formation, and (2) formation pore pressure changes in response to flow toward the zero pressure boundary of the excavation. (If heating of the test interval fluid was the cause of the initial pressure rise, its cooling would only return the pressure to its pre-excavation value.) The pressure response to dilation will occur relatively quickly, whereas the pressure changes in response to flow in a low permeability medium such as rock salt will happen more slowly. The test interval responses are consistent with a dilatant zone surrounding the large-diameter borehole out to about 1.5 r. In this region, there appears to be sufficient increase in pore volume so that brine-filled test intervals almost immediately lose nearly all of their pressure. Relatively large increases in pore volume may not be able to be instantaneously saturated by brine from the surrounding low permeability formation. The gas-filled test intervals at 1.25 r also

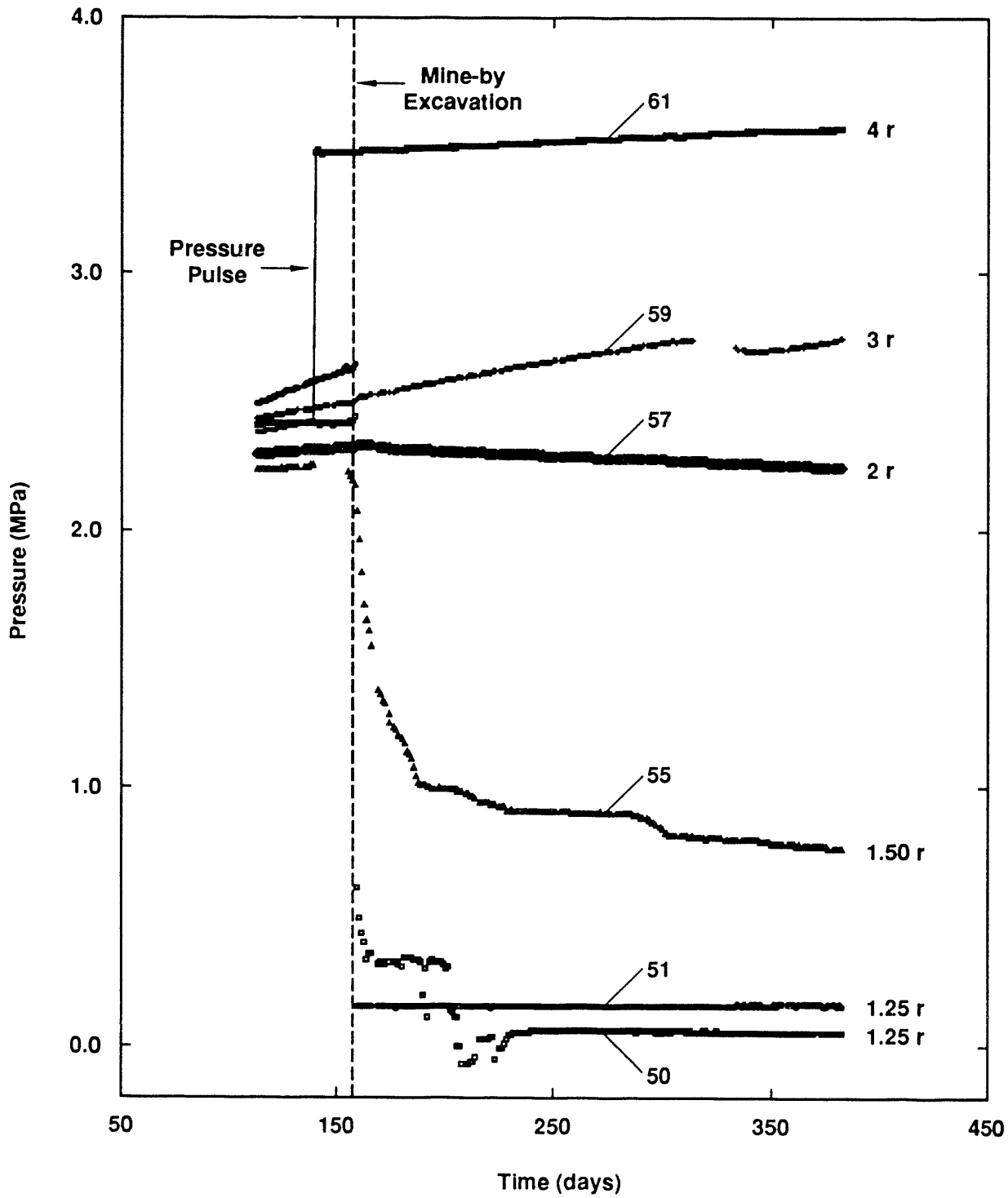

Figure 10: Pressure-time data from gas-filled test intervals during and following excavation.

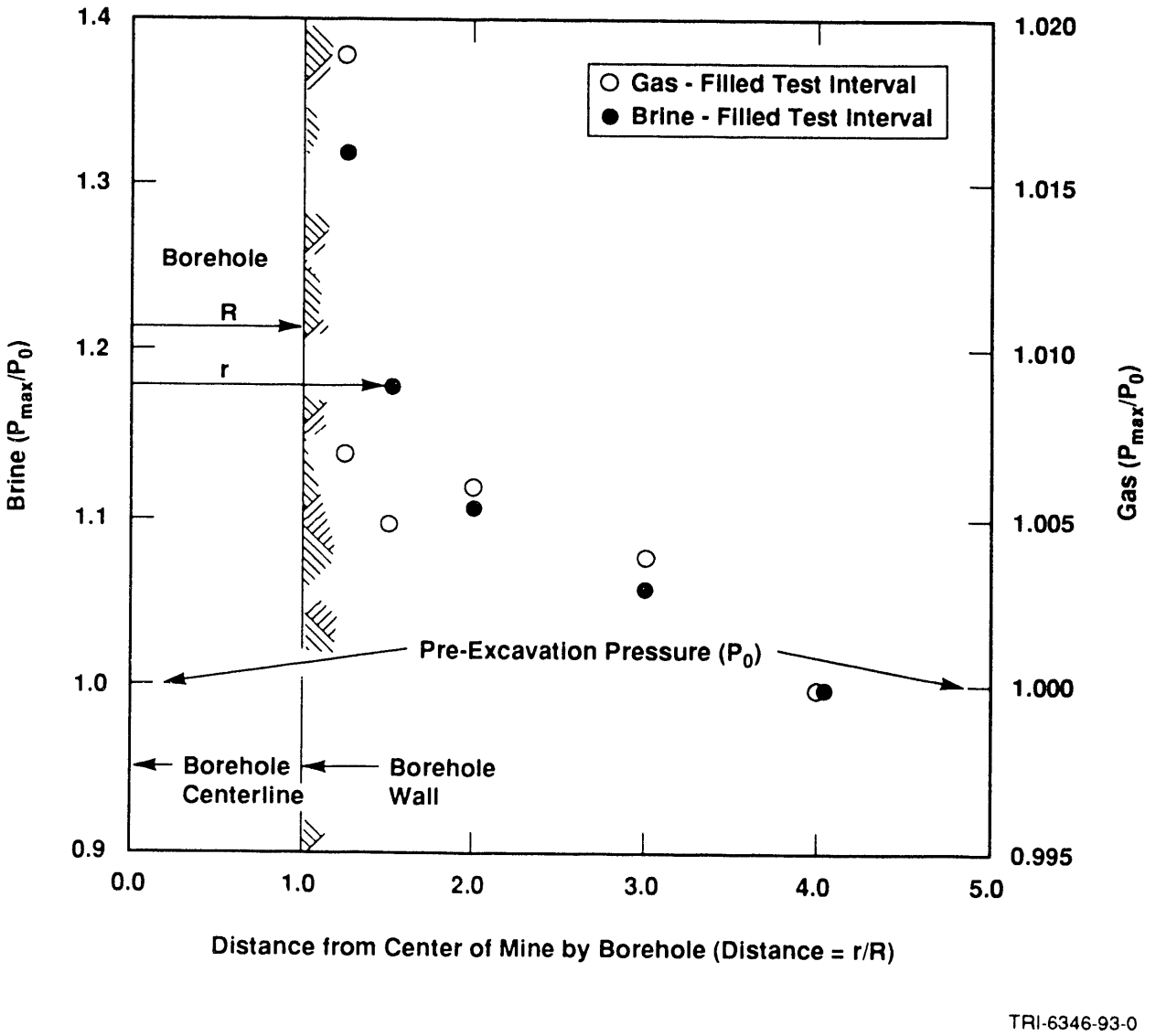

Figure 11: Peak pressures normalized to pre-excavation pressure at time of mine-by drilling.

lose virtually all of their pressure. In order for this to happen, the formation has to become undersaturated with respect to brine. At 1.5 r, the gas pressure decreases from over 2 MPa and stabilizes at 0.7 MPa, indicating that some gas flowed out of the borehole into the formation and then stopped. If the formation pressures are symmetric about the excavated borehole, the brine-filled test interval response indicates that the the formation pressure is zero at 1.5 r. The equilibrium pressure of 0.7 MPa in the gas-filled test interval at 1.5 r, therefore, may be a measure of a displacement or threshold pressure in the disturbed region.

Beyond 1.5 r, the changes in response to excavation are less dramatic. The pressure responses of the brine-filled test intervals to excavation decrease with distance from the large-diameter borehole. In the gas-filled test interval at 2 r, the slow decrease in the test interval pressure suggests that the formation pressure at this location has reduced below the test interval pressure. Either the gas pressure is sufficient to overcome the threshold pressure, or the brine which has accumulated in the test interval during the pre-excavation inflow period is forced into the formation. Beyond 2 r, the gas-filled test intervals are not affected by the excavation.

Formation pore pressure changes are not immediately manifested as pressure changes in the test intervals due to the slow movement of fluid in the low-permeability formation and the relatively great fluid storage volume in the test intervals. With time, however, the test interval pressures will approach the adjacent formation pressure. Therefore, the brine-filled test interval pressure approaching an equilibrium more than 200 days after the mine-by should be representative of a pore pressure in the formation.

The equilibrium pressures in the gas-filled test intervals at 1.5 r and beyond (Figure 10) are greater than those in the brine-filled test intervals at a comparable distance (Figure 9). If the pore pressures are symmetric about the large-diameter hole, then the difference in pressures in the gas- and brine-filled test intervals may be a measure of capillary pressure effects.

4.3 Post-excavation injection tests

Approximately 240 days after excavation, injection tests were conducted in the test intervals. The formation properties were estimated from the injection test by means of numerical simulations. The equilibrium pressure immediately prior to each injection test is taken as the constant formation pressure. Because all of the brine-injection tests were constant-pressure flow tests, the test interval compressibility does not affect the measured response and is not required as input to the numerical simulation. Test interval closure is not considered because of the relatively short test duration. Permeability and porosity are the remaining free parameters; they are adjusted until a reasonable agreement between the numerical simulation and the measured response is obtained.

Table IV: Summary of Brine-Injection Test Results

Borehole number	Position (r)	Permeability (m^2)	Porosity
52	1.25	$5.7x10^{-18}$	0.01
53	1.25	$5.7x10^{-18}$	0.01
54	1.5	$1.5x10^{-19}$	0.005
56	2.	$1.8x10^{-20}$	0.001
58	3.	$4.5x10^{-21}$	0.001
60	4.	$5.5x10^{-21}$	0.001

All of the injection tests in the brine-filled test intervals were constant-pressure injection tests. The pressures in both test intervals at 1.25 r were increased 0.45 MPa above the previous pressures; the pressures in the remaining test intervals were increased 0.7 MPa over the previous pressures. The results are summarized in Table IV, and the injection data and the best-fit numerical simulations are given in Figures 12 through 17.

For all of the tests in the brine-filled test intervals, the injection rates are greatest initially and level off to nearly constant values for the remainder of the tests. The numerical simulations do not reproduce the initial faster rates, and the matches are based on the later, nearly constant rate. The initial response may be a result of the same factors discussed in Section 4.1 regarding the relatively fast brine-pulse decay in borehole 60: test system compressibility, mechanical-hydrologic coupling, and/or a local DRZ.

Examples of the sensitivity of the calculated response to the assumed values of permeability and porosity are given in Figure 14. The calculated response is considerably more sensitive to the value of permeability than porosity, consistent with the interpretation of the pre-excavation build-up data.

Remarkably, the injection tests in both brine-filled test intervals at 1.25 r yielded interpreted permeabilities of $5.7x10^{-18}$ m^2 and porosities of 0.01. The permeabilities and porosities interpreted from the brine-injection tests decreased as the distances from the mine-by borehole increased. At 1.5 r, a permeability of $1.5x10^{-19}$ m^2 and a porosity of 0.005 were determined from the injection data. A permeability of $1.8x10^{-20}$ m^2 and a porosity of 0.001 were determined from the injection tests at 2 r. At 3 r and 4 r, the interpreted permeabilities and porosities were comparable to those before excavation ($5x10^{-21}$ m^2, 0.001), indicating that the excavation had no measurable effect on the brine permeability at 3 r and beyond.

The gas-injection test results are summarized in Table V. The injection data and

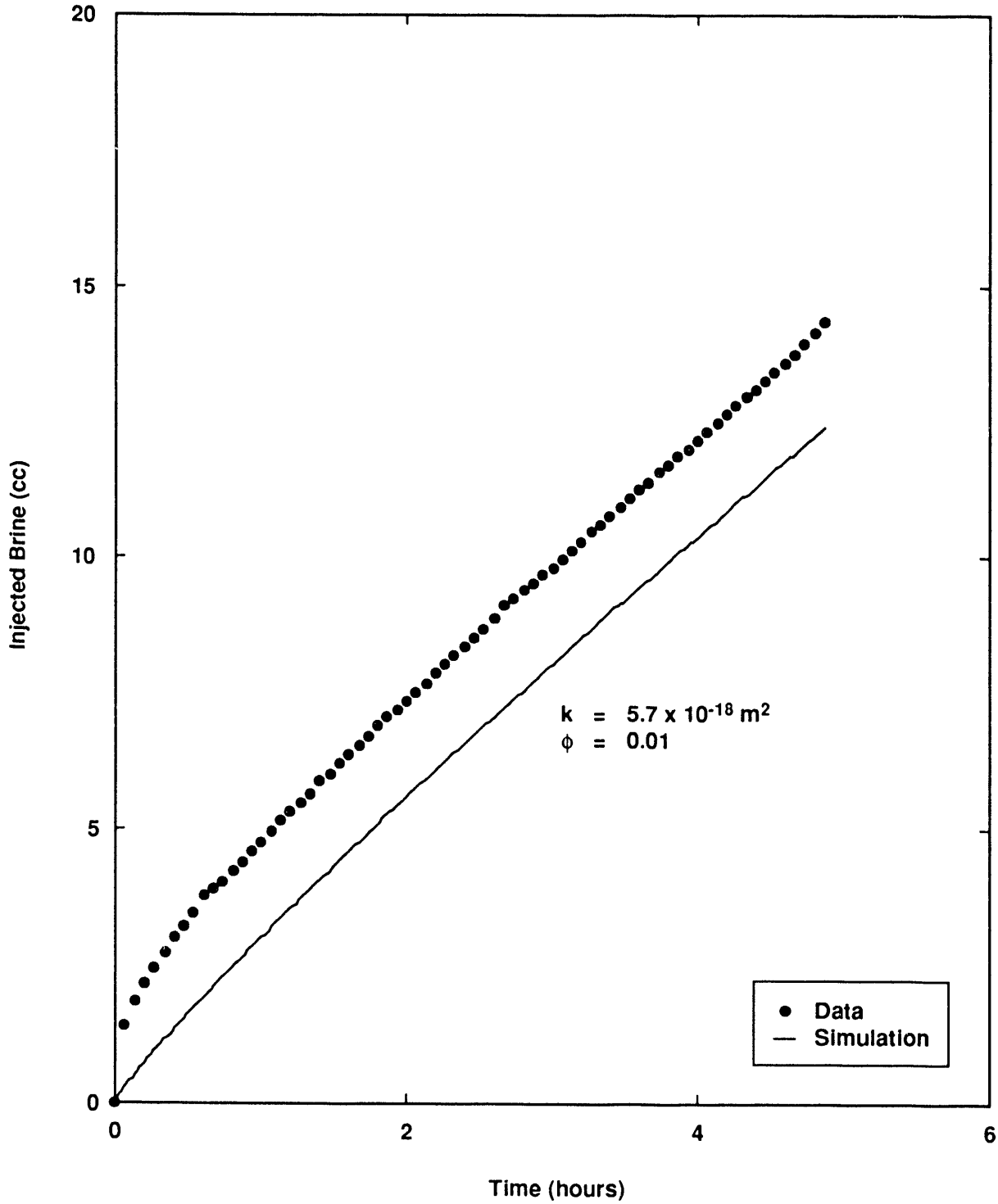

Figure 12: Results from and numerical simulation of brine-injection test at 1.25 r in borehole 52.

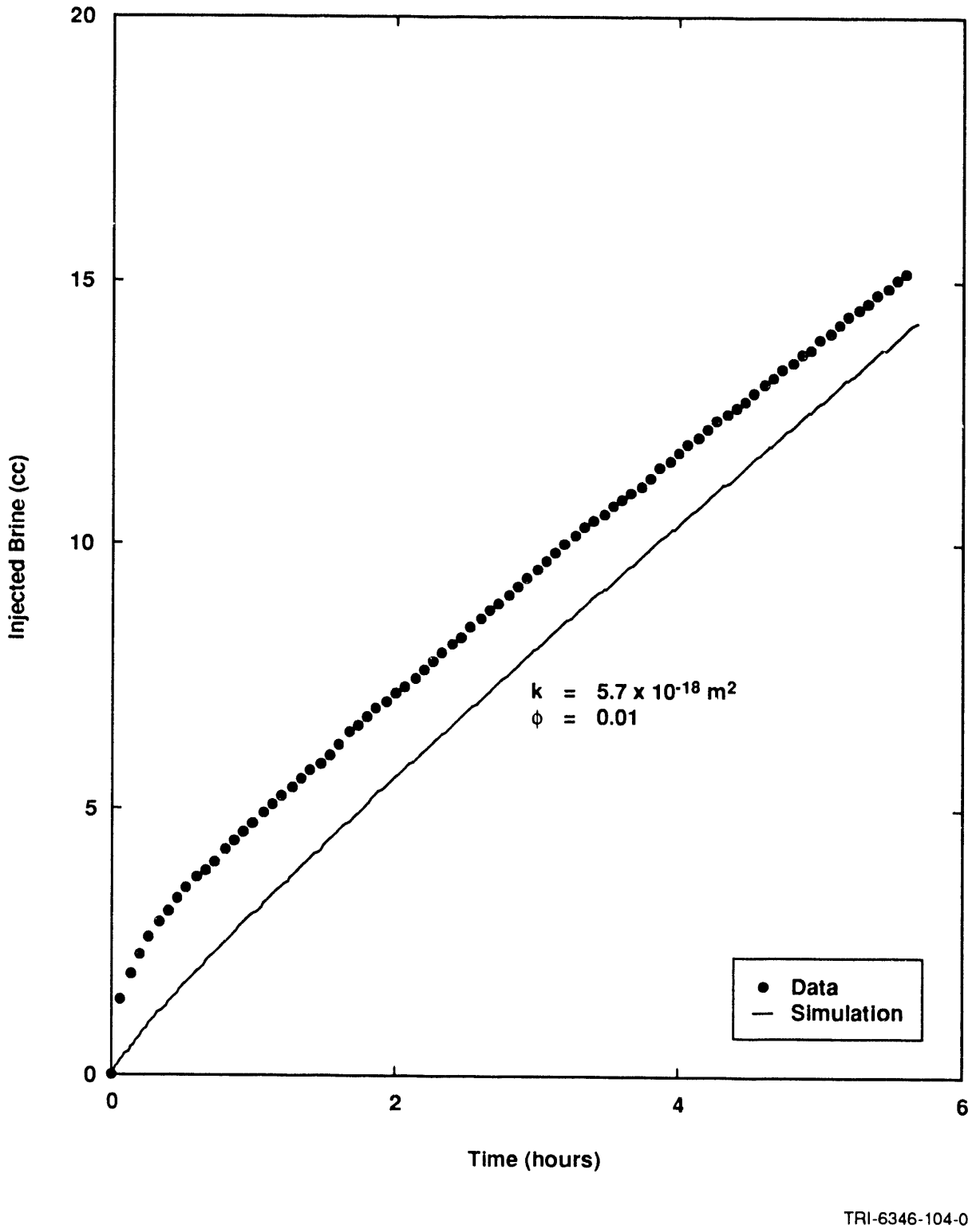

Figure 13: Results from and numerical simulation of brine-injection test at 1.25 r in borehole 53.

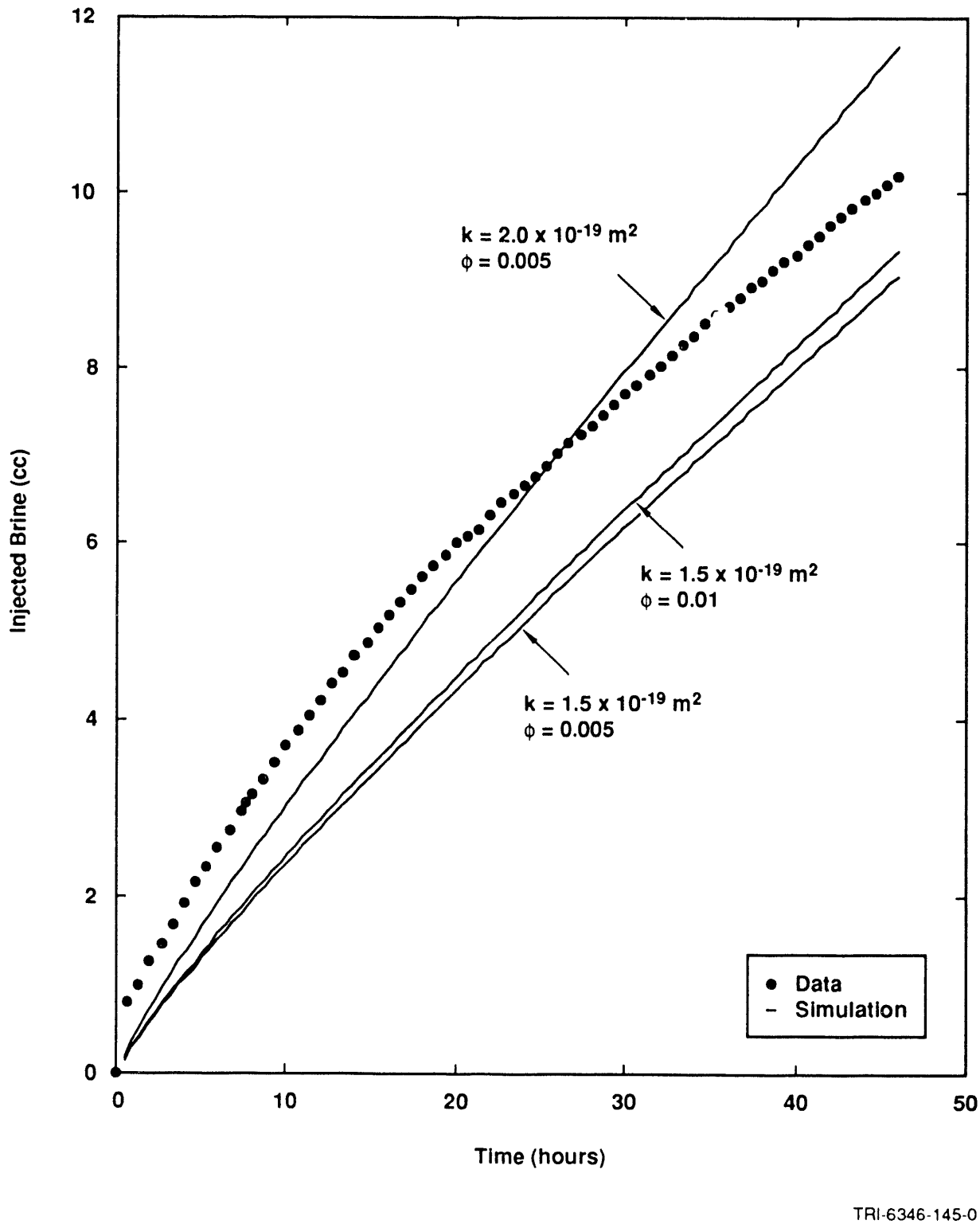

Figure 14: Results from and numerical simulations of brine-injection test at 1.5 r in borehole 54.

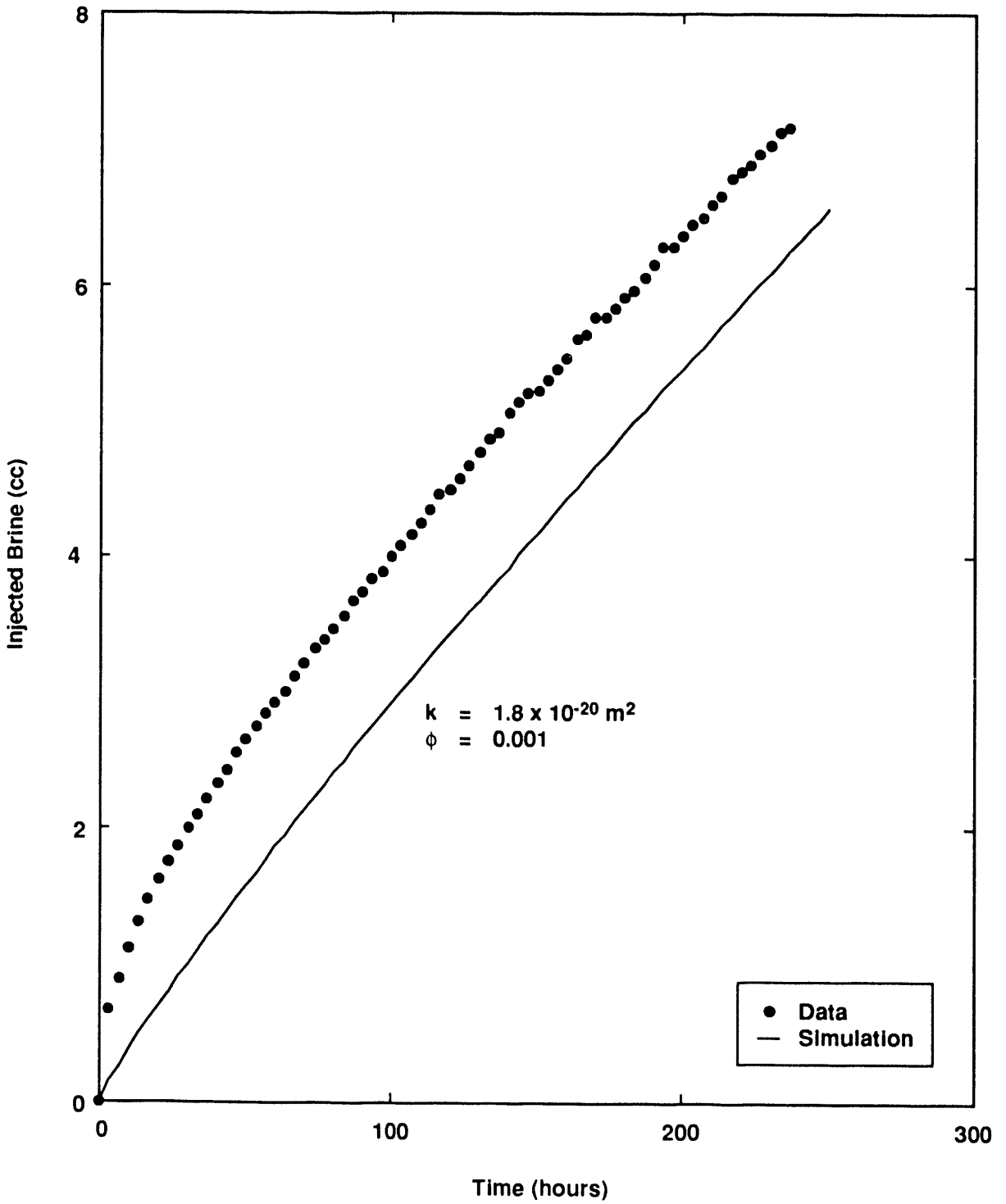

Figure 15: Results from and numerical simulation of brine-injection test at 2 r in borehole 56.

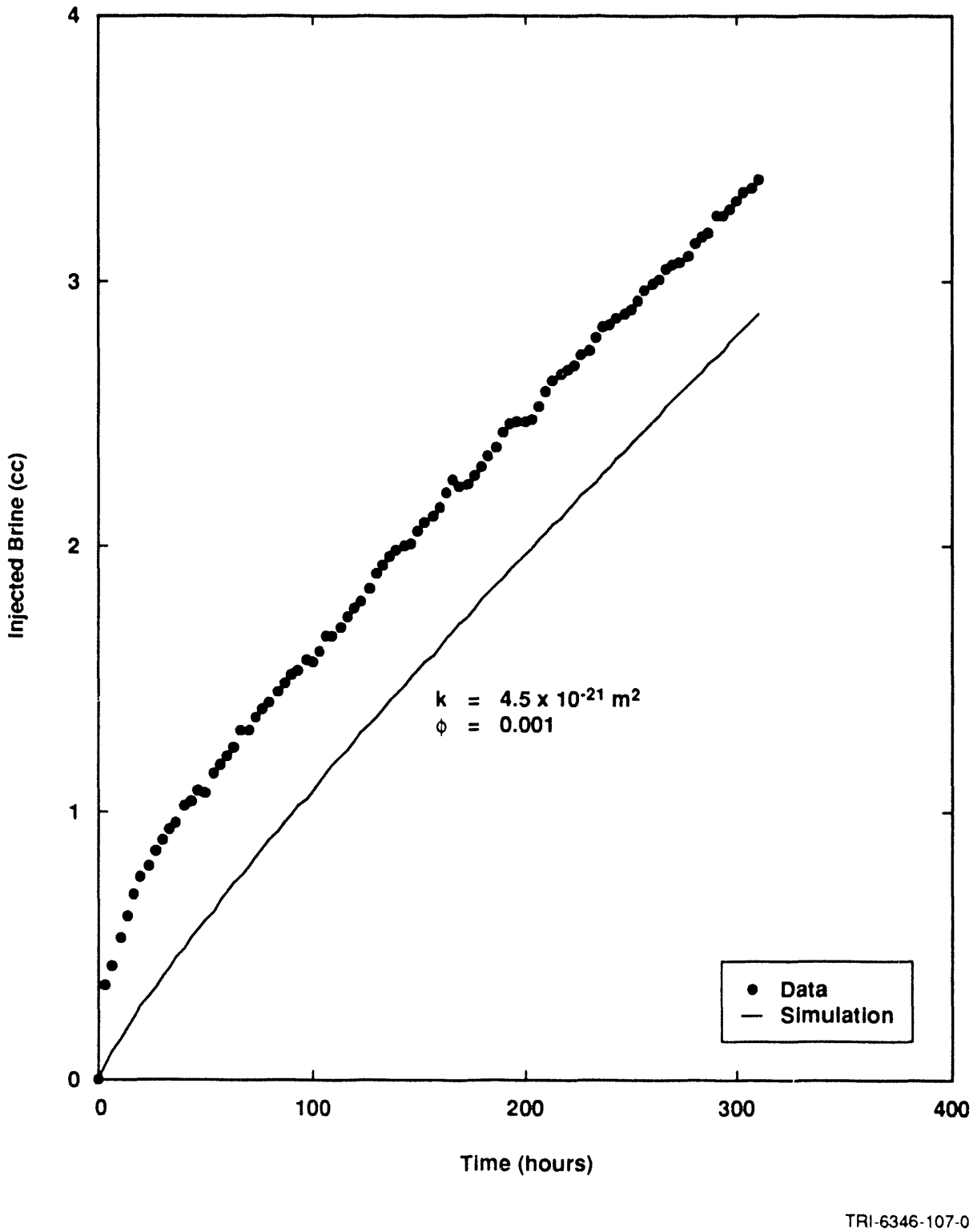

Figure 16: Results from and numerical simulation of brine-injection test at 3 r in borehole 58.

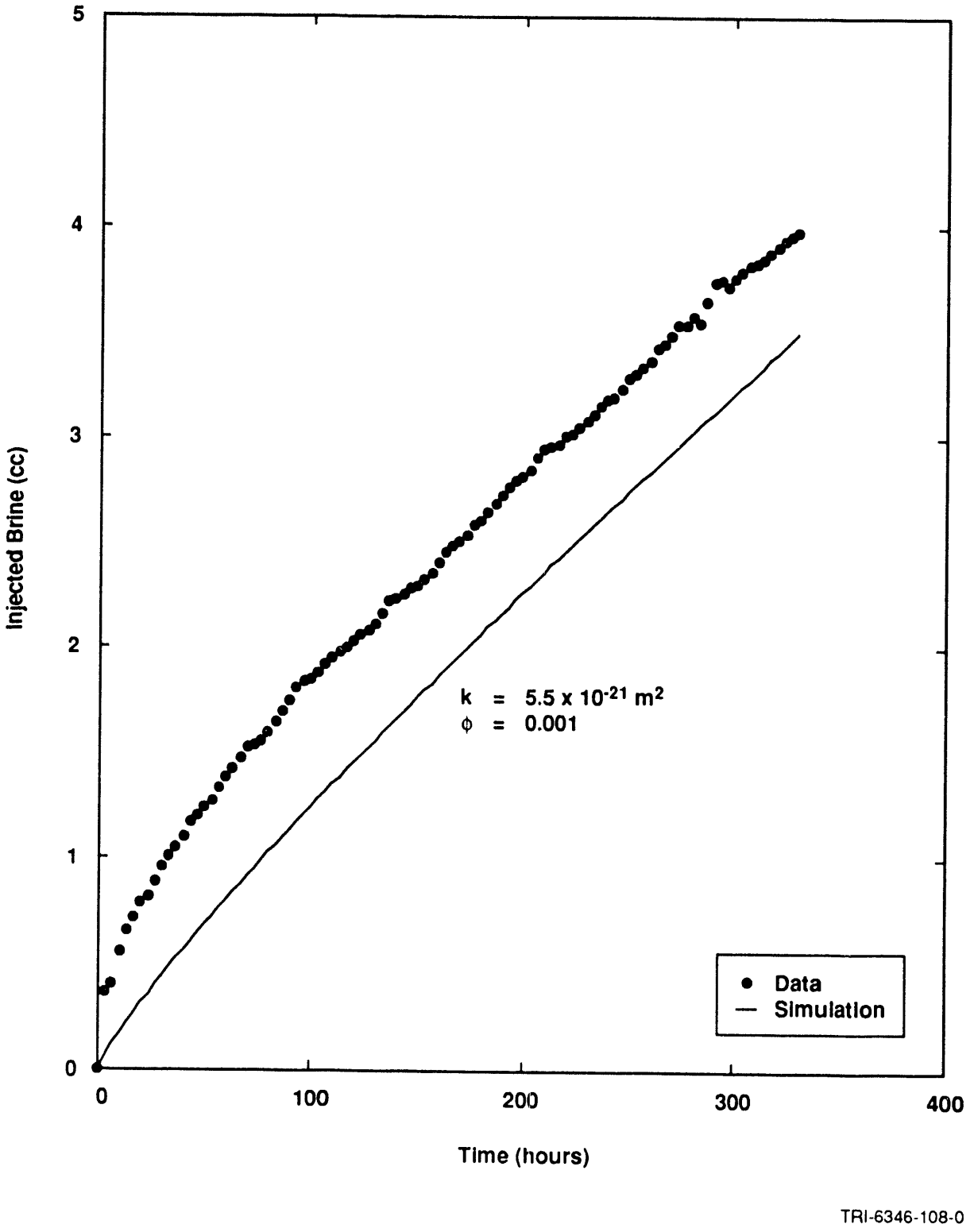

Figure 17: Results from and numerical simulation of brine-injection test at 4 r in borehole 60.

best fit numerical simulations are given in Figures 18 through 22. In the two gas-filled test intervals at 1.25 r, constant-pressure (0.24 MPa) injection tests were conducted. The relatively fast flow of gas from the test intervals, coupled with the fact that these test intervals had lost all of their pressure in response to the mine-by, indicates that the formation surrounding these test intervals is partially saturated. Therefore, these test data were interpreted as gas flowing into gas-filled porosity; the permeabilities interpreted from these data were 9.0×10^{-16} m^2 and 4.5×10^{-18} m^2, both with porosities of 0.01. The constant-pressure test in borehole 50 is used to illustrate the sensitivity of the calculated response to the assumed values of permeability and porosity. As before, the calculated response is more sensitive to the value of permeability compared to porosity.

In the gas-filled test intervals at 1.5, 2, and 3 r, pressure-decay tests were conducted by increasing the test interval pressures by 1.4 MPa over the previous pressure and shutting the test intervals in. For the gas-injection test at 1.5 r (Figure 20), the volume of gas which moves from the test interval into the formation during the injection test is in excess of 300 cm^3, and it is clear that gas is extending an appreciable distance into the formation. We modeled the flow induced by this test in two fundamentally different ways. One model assumes gas flow into a gas-filled porosity. In other words, the formation is assumed to be partially saturated and the gas travels only in the gas-filled portion of the porosity. For this assumption, the interpreted gas permeability and porosity are 2.0×10^{-21} m^2 and 0.001, respectively. The other model assumes the gas in the test interval displaces or drives brine flow in the formation, as if the rock surrounding this borehole remained saturated but at a low enough pressure so gas can displace the brine. Simulations with this model do not model two-phase flow, but assume that the brine flow in the formation controls the flow and the corresponding test interval response. In this case, the interpreted brine permeability and porosity are 2.0×10^{-19} m^2 and 0.005, respectively. Only a single calculated pressure-time history is given in Figure 20 because the two different simulations produce identical responses.

For the gas-injection test at 1.5 r, it is more likely that the gas is driving brine flow as opposed to gas flowing through a partially saturated formation for a number of reasons. First, the uneven or step-wise pressure history during the shut-in test is consistent with that expected during viscous fingering or channeling (Dullien, 1979). This phenomenon occurs when the viscosity of the displacing fluid is less than that of the saturating fluid, as is the case for gas displacing brine. The advancement of the gas into the pores will be uneven because pore size distribution is heterogeneous; consequently, the gas pressure changes in the test interval in response to this flow will be uneven. Second, the brine-injection test at the same distance into the formation (1.5 r) results in an interpreted permeability of 1.5×10^{-19} m^2 and a porosity of 0.005 (Table IV), consistent with the values obtained assuming gas-driven brine flow in the formation. Finally, recall that this test interval maintained some pressure after excavation (Figure 10); if a continuous gas-filled porosity surrounded this borehole, the test interval would be expected to lose

all of its pressure.

Table V: Summary of Gas-Injection Test Results

Borehole number	Position (r)	Permeability (m^2)	Porosity
50	1.25	$4.5x10^{-18}$	0.01
51	1.25	$9.0x10^{-16}$	0.01
55 *	1.5	$2.0x10^{-19}$	0.005
57 *	2.	$3.0x10^{-21}$	0.001
59 *	3.	$6.0x10^{-21}$	0.001
61**	4.	NO TEST	NO TEST

* Tests were interpreted as the test interval gas driving brine flow in the formation.
** Pulse test conducted prior to excavation.

At distances of 2 r and greater, the gas shut-in tests resulted in very small pressure decays. If these data are interpreted in terms of flow in gas-saturated porosity, the corresponding permeabilities would be much less than 10^{-22} m^2, so small as to doubt they are measurable. It is more plausible that the gas pressure is forcing brine out into the formation. In this case, the interpreted permeabilities are in the reasonable range of 10^{-20} to 10^{-21} m^2. Comparable values were determined from the injection tests in the brine-filled test intervals at similar locations (Table IV). In both tests, it was not possible to exactly match the measured response. At 2r, the pressure-decay rate decreases midway through the test. At 3r, the pressure-decay rate decreases after a pressure decrease induced during a borehole volume measurement.

There is some question as to the nature of the flow induced by the gas-injection tests at 2 r and 3 r. The flow of gas is so small during these injection tests (a few cm^3) that it is not possible to determine if the gas actually moves into the formation. Perhaps gas is displacing brine in the formation, but only in a small zone of enhanced permeability surrounding the test intervals. An alternative explanation is that brine which was produced into the test interval during the pre-excavation inflow phase is now being forced back out into the formation.

The injection test results can be summarized as follows. At 1.25 r, the formation is largely unsaturated, and both gas and brine can be injected into the formation at rates which correspond to permeabilities of $5x10^{-18}$ m^2 or greater. At 1.5 r, the formation is depressurized, but probably nearly completely saturated, and gas can be injected into the formation and displace the formation brine. The permeability at this location is $2x10^{-19}$ m^2. Beyond 1.5 r, there is no measurable permeability to gas. The brine permeability continues to decrease so that at 2 r, it is about $2x10^{-20}$ m^2. At 3 and 4 r, the brine permeability is comparable to that before excavation ($\sim x10^{-21}$ m^2).

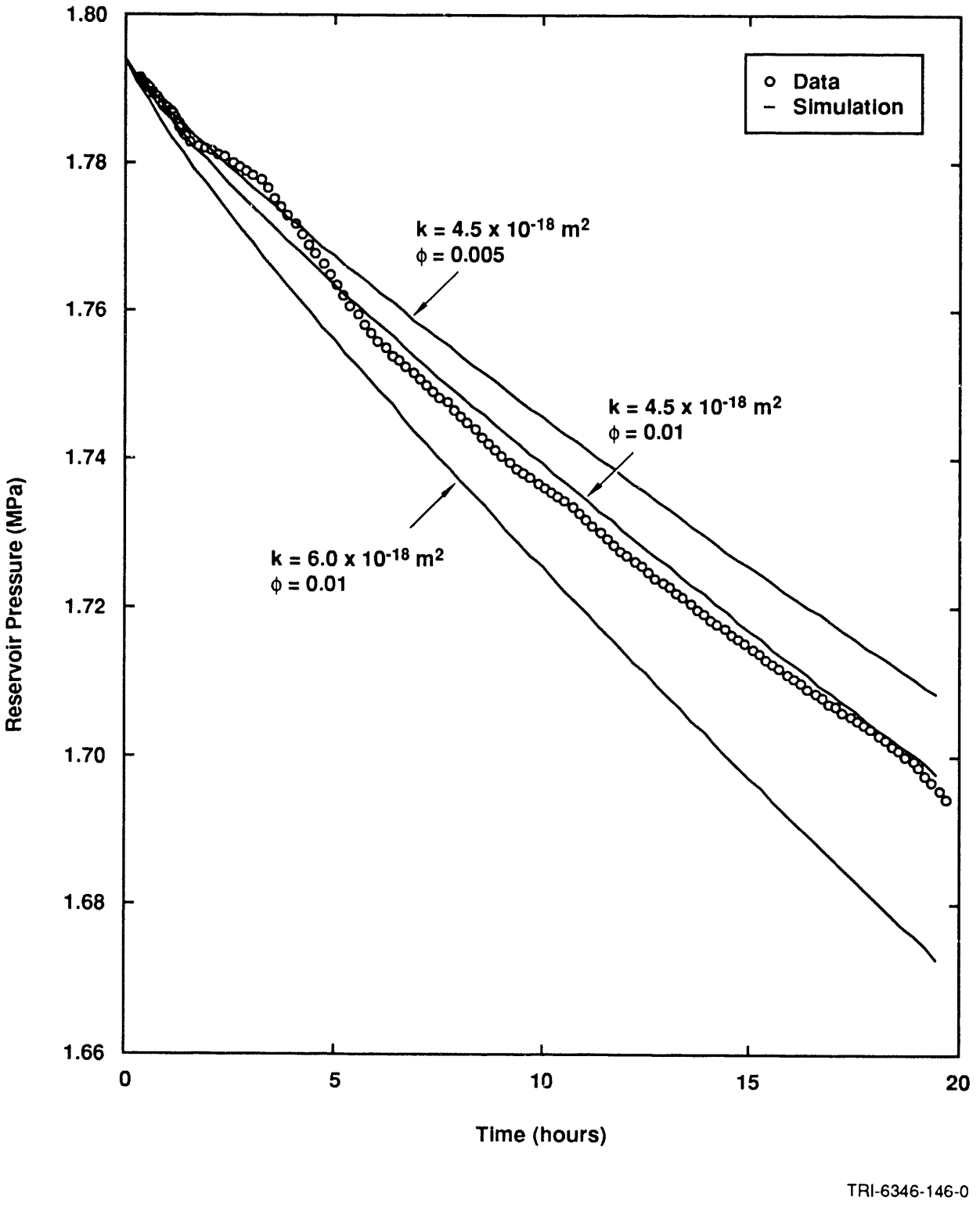

Figure 18: Results from and numerical simulations of gas-injection test at 1.25 r in borehole 50.

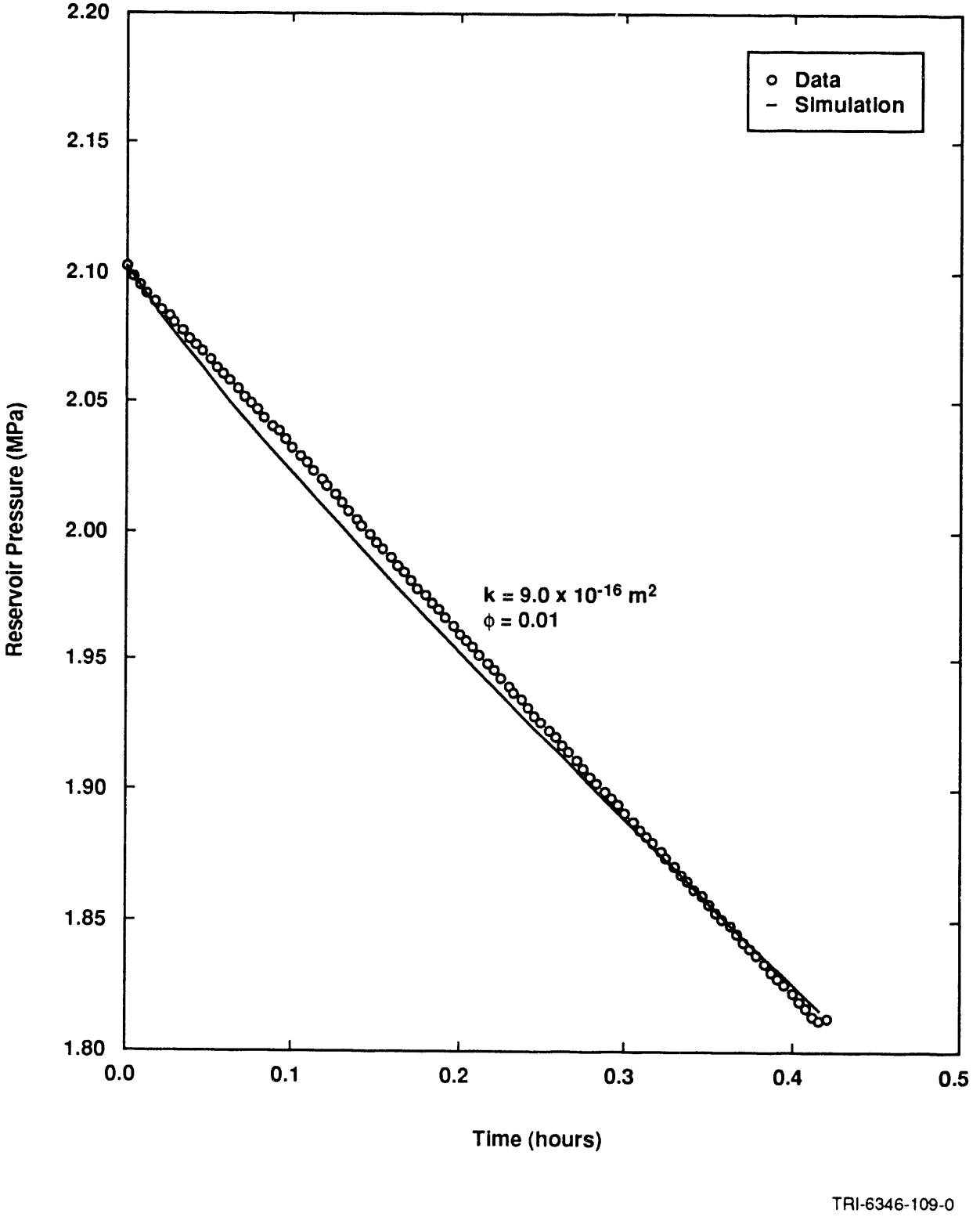

Figure 19: Results from and numerical simulation of gas-injection test at 1.25 r in borehole 51.

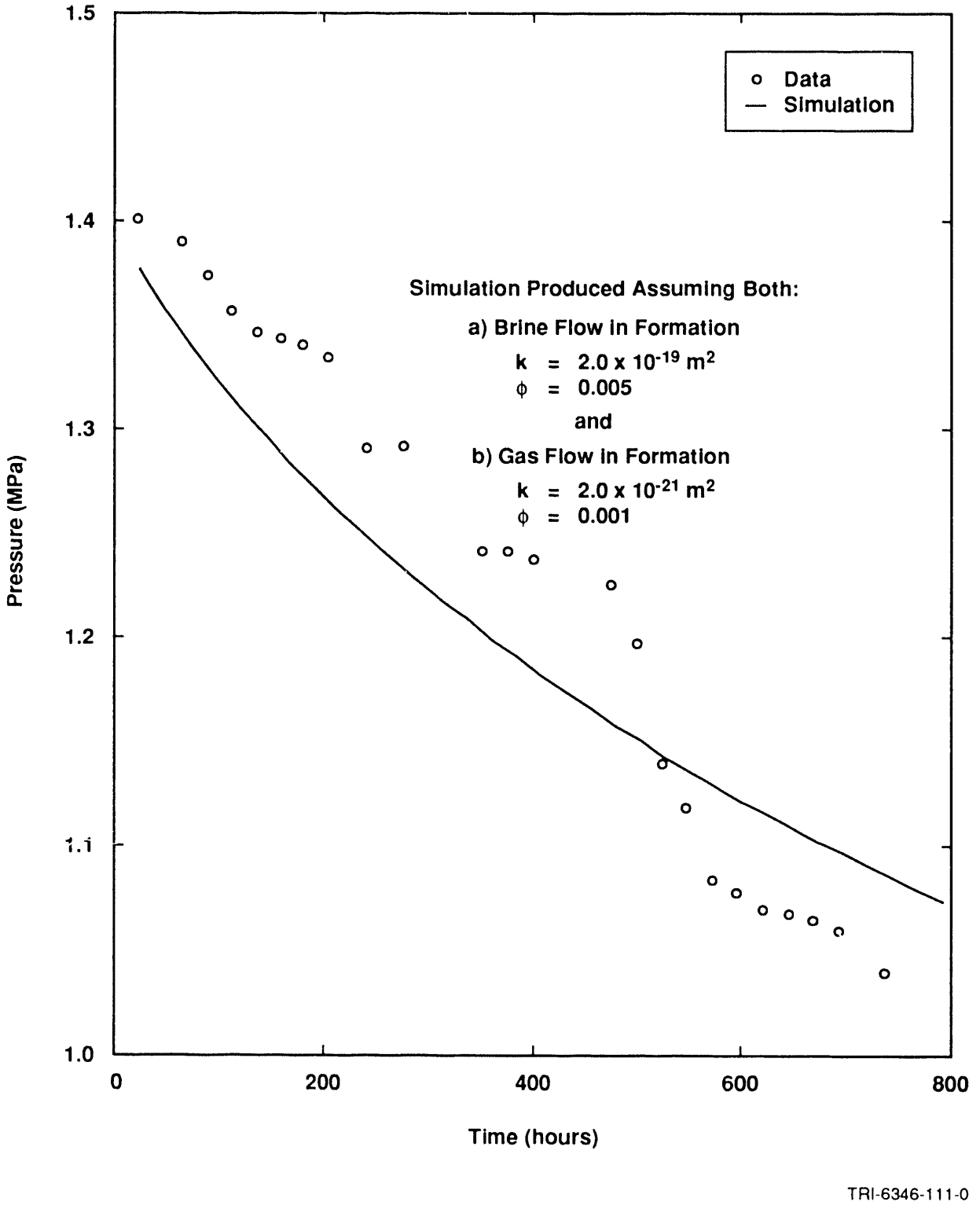

Figure 20: Results from and numerical simulation of gas-injection test at 1.5 r in borehole 55.

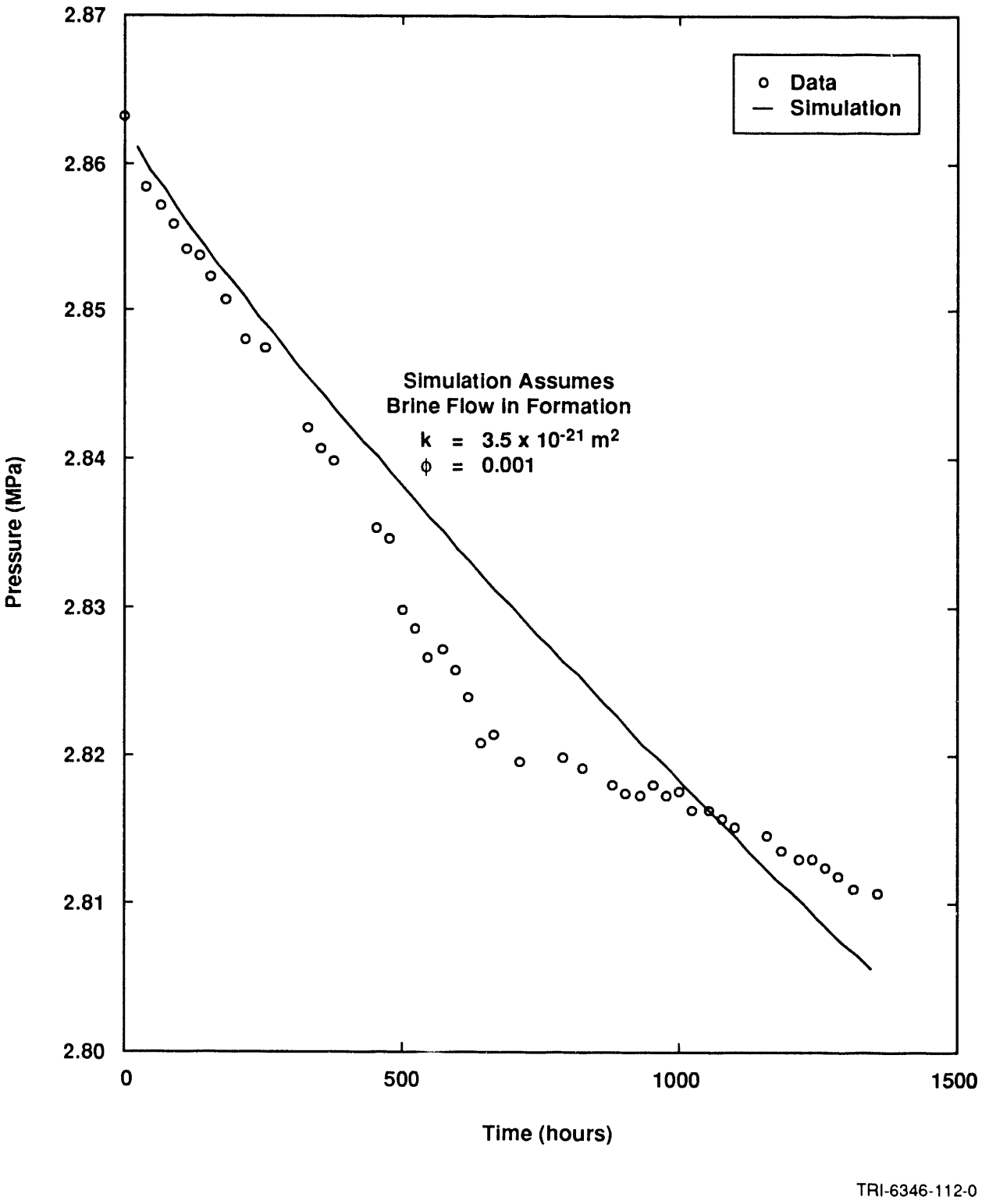

Figure 21: Results from and numerical simulation of gas-injection test at 2 r in borehole 57.

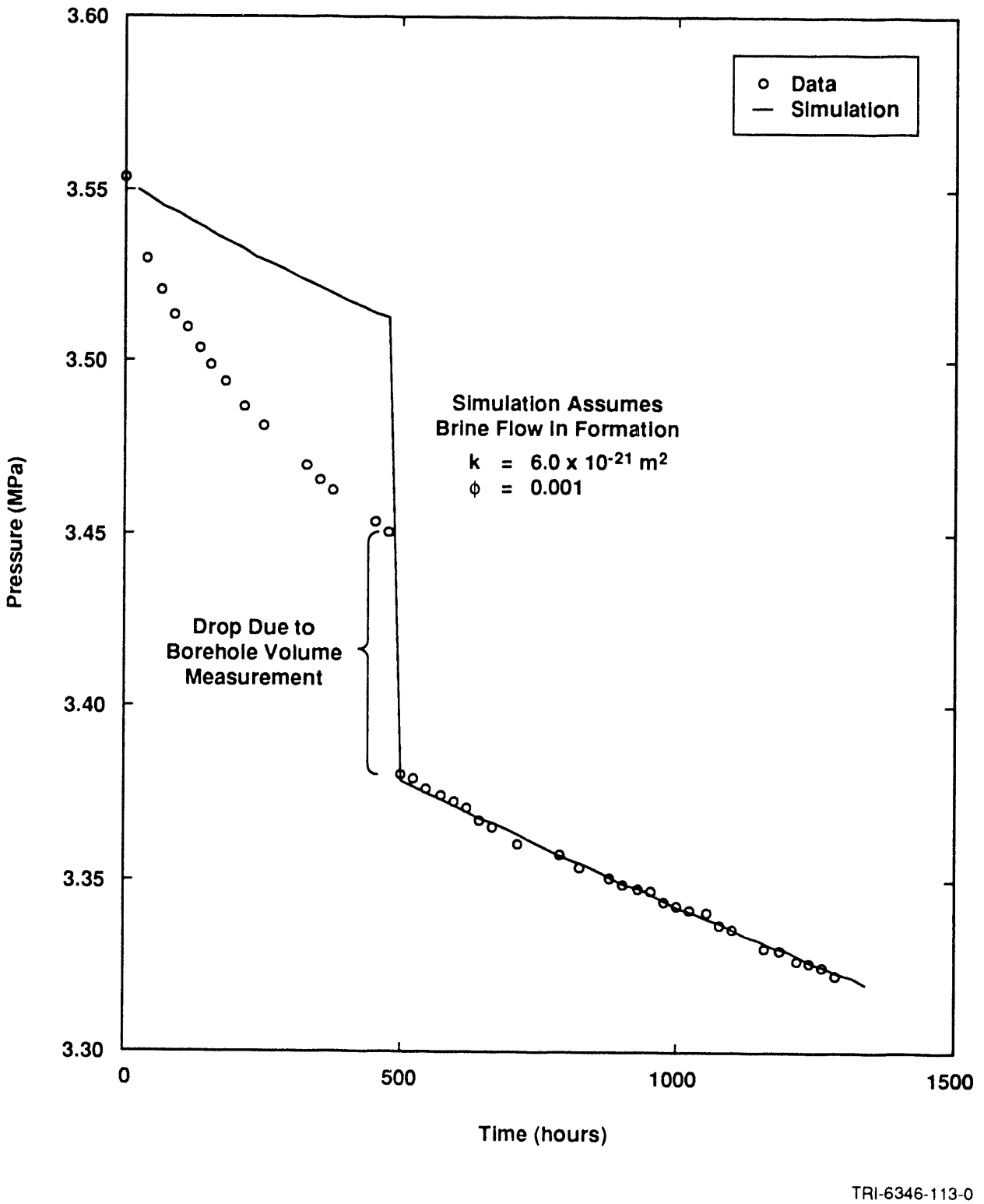

Figure 22: Results from and numerical simulation of gas-injection test at 3 r in borehole 59.

5 Discussion

The test results reveal that hydrologic parameters (properties and response) of the formation are altered in the vicinity of the mine-by excavation. As shown in Table VI, the magnitude and extent of the effect at the time they were estimated depend on which hydrologic parameter is considered.

Table VI: Hydrologic Parameters Affected by Mine-By (as estimated 240 days after excavation)

Parameter	Approximate depth influenced (r)
Gas permeability	1.25
Brine permeability	2.0
Saturation	1.25
Porosity	1.5
Pore pressure	3.0

The previous definition of the DRZ has been a qualitative, non-specific term which indicates that some formation properties have been altered in response to excavation. A more fundamental definition of the DRZ is the volume of rock which experiences a change in its pore structure in response to excavation. Defining the DRZ in terms of pore structure changes allows physical insight into the response of the rock mass. Pore structure is the link between the mechanical and hydrologic response of a porous medium. For example, an increase in mean stress tends to close existing pores and cracks; this closure, in turn, reduces the connnected porosity and permeability. To predict permeability or permeability changes from a fundamental basis, a model or representation of pore structure must be used.

Pore structure can be altered in two fundamental ways: changes in the existing pore structure and creation (or deletion) of pore structure. Most pore structure models concern changes in the existing pore structure. For example, models which relate permeability and mean stress have been developed by assuming elastic, recoverable deformation of the existing pore structure (e.g., Walsh, 1981; Gangi, 1978; Ostensen, 1983). Creation of new porosity, such as in the DRZ, will also induce permeability changes. These permeability changes are due in part to deviatoric stresses, and may or may not be recoverable.

A conceptual model of pore structure changes in the rock surrounding the mine-by borehole is given in Figure 23. The rock mass is defined in terms of three regions. In the first region adjacent to the excavation, the rock is the most damaged (major DRZ).

The damage is manifested principally as grain boundary microcracking accompaned by dilation (Stormont, 1990b), and is a result of relatively high deviatoric and low hydrostatic stresses induced by the excavation. This damage does not imply failure or loss of strength of the rock salt. With increasing distance from the excavation, the stresses are less favorable for damage. The second region contains a combination of damage with little dilation and changes in the existing pore structure (minor DRZ). The first and second region comprise the DRZ. Beyond some distance from an excavation, there is no significant effect of the excavation on the pore structure (neglecting the very small elastic and unknown time-dependent response of the pore structure). This so-called undisturbed region is still affected by the excavation, and processes which do no require pore structure changes such as isovolumetric creep and pore pressure changes occur in this region as well as in the DRZ.

Pore structure damage is responsible for the majority of the effects attributed to the DRZ in rock salt. When accompanied by dilation, damage reduces the pore pressure and may induce a partially saturated state. Measurable gas permeability is possible under these conditions. Brine permeability will be increased due to the increased size and connnectivity of the damage-induced pore structure. Damage increases the effective or bulk compressibility of a material, not only decreasing the effective elastic moduli but also increasing its hydraulic storage capability of the material.

The experimental results summarized in Table VI are consistent with the concept that pore structure changes alter the hydrologic properties of rock salt. Gas permeability probably only exists in the region which has experienced substantial damage, and will be nearly coincident with the limit of partial saturation. Brine permeability will be affected by changes in the existing pore structure, and these effects will therefore extend beyond the depth of measurable gas permeability to the limit of the DRZ. Pore pressure changes do not require pore structure change, and can therefore extend outside of the DRZ.

The results of the mine-by experiment substantiate the use of gas flow tests to measure or delineate the major DRZ. We found that intact, saturated rock salt has an immeasurably small permeability to gas. In contrast, in the region adjacent to the excavation which is depressurized and probably partially saturated, gas can be injected into the formation. The most plausible mechanism for the development of this region is pore structure damage and dilation. Thus, successful gas flow tests indicate regions which have experienced damage and constitute the major component of the DRZ.

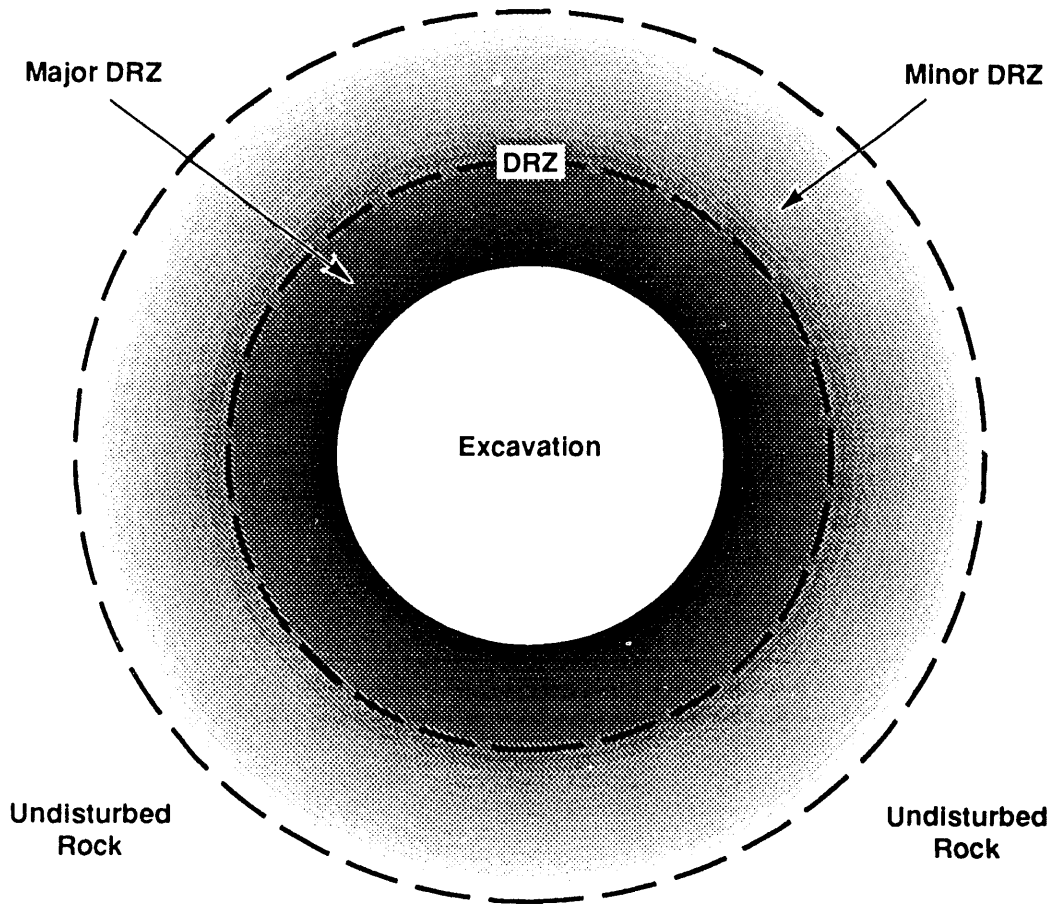

Major DRZ	Minor DRZ
• Due to Damage and Dilation as well as Changes in Existing Pore Structure	• Due to Changes in Existing Pore Structure and Limited Damage and Dilation
• Measurable Gas Permeability	• No Measurable Gas Permeability Due to Great Threshold Pressures
• Relatively Great Brine Permeability	• Some Increase in Brine Permeability
• Low Pore Pressure • Partial Saturation	• Some Pore Pressure Decrease Due to Dilation, but Remains Saturated

TRI-6346-92-0

Figure 23: Conceptual model of pore structure changes in rock surrounding an excavation

6 Summary

The mine-by experiment provides direct evidence of changes in hydrologic parameters of rock salt as a result of nearby excavation. The results are summarized in Figure 24. Prior to mine-by excavation, formation fluid (presumably brine) flows into both the brine-filled and gas-filled test intervals. Interpretations of the pressure build-ups yield permeabilities on the order of 10^{-21} m^2 and a formation pore pressure of about 3 MPa. Gas does not flow into the formation, even when the gas pressure equals or exceeds the formation pressure. At these conditions, the formation has no measurable permeability to gas.

The mine-by excavation induces dramatic changes in the hydrologic parameters of the formation. Concurrent with excavation, a desaturated zone is created out to a distance from the excavation of 1.25 to 1.50 r. Beyond 1.5 r, the formation remains saturated. A pore pressure gradient develops from near zero at 1.5 r to about 3 MPa at 4 r.

The gas and brine permeabilities, as determined by injection tests, are also altered as a result of the excavation. The injection measurements in the brine-filled test intervals indicate a gradient of brine permeabilities as the distance from the excavation increases: from as high as $5x10^{-18}$ m^2 at 1.25 r to near the pre-excavation value at 3 r ($5x10^{-21}$ m^2). Gas can readily be injected into the partially saturated formation at 1.25 r, corresponding to a gas permeability of $5x10^{-18}$ m^2 and greater. At 1.5 r, gas can be injected into the formation, but it is most likely displacing formation brine rather than flowing through gas-saturated porosity. Beyond 1.5 r, there is no measurable gas permeability.

The test results reveal that the extent and magnitude of the (hydrologic) DRZ depends on which parameter is considered. The greatest changes in hydrologic parameters are confined to 1.5 r, and are asssociated with pore structure damage. Defining the DRZ in terms of pore structure change and damage provides a framework for gaining physical insight into the processes active in the development of the DRZ and may aid in developing the fundamental relationship between mechanical and hydrologic behavior of rock salt.

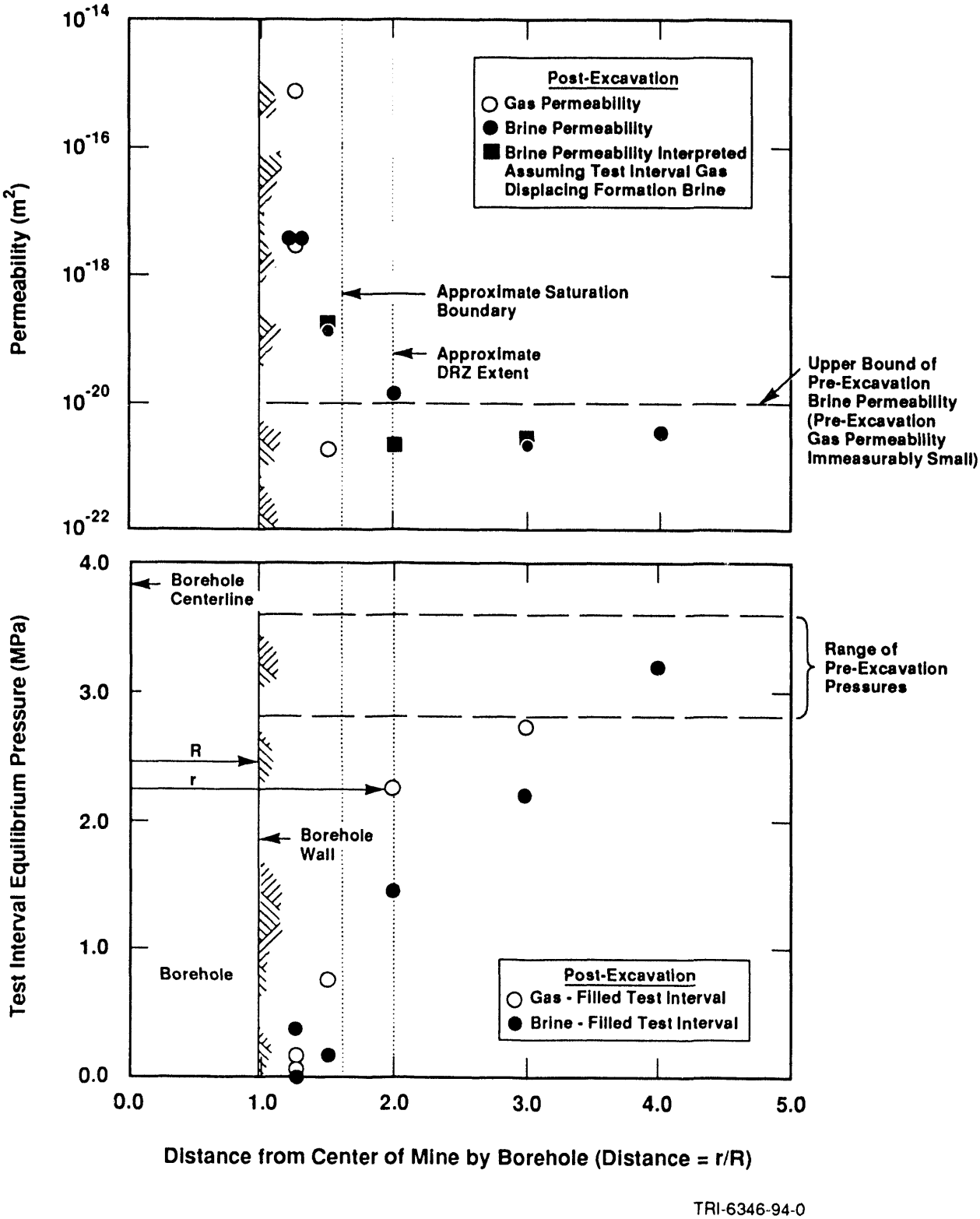

Figure 24: Summary of Pre-and Post-Excavation Results.

7 References

R. L. Beauheim, G. J. Saulnier, Jr. and J. D. Avis, 1991, "Interpretation of Brine-Permeability Tests of the Salado Formation at the Waste Isolation Pilot Plant Site: First Interim Report," Sandia National Laboratories report in preparation.

D. J. Borns and J. C. Stormont, 1988, "An Interim Report on Excavation Effect Studies at the Waste Isolation Pilot Plant: Delineation of the Disturbed Rock Zone," Sandia National Laboratories report SAND87-1375.

J. P. Carter and J. R. Booker, 1990, "Sudden Excavation of a Long Circular Tunnel in Elastic Ground", International Journal of Rock Mechanics, Mining Science & Geomechanics Abstracts, Vol. 27, No. 2, p. 129-132.

F. A. L. Dullien, 1979, Porous Media: Fluid Transport and Pore Structure, Academic Press, New York.

A. F. Gangi, 1978, "Variation of Whole and Fractured Porous Rock Permeability with Confining Pressure," International Journal of Rock Mechanics and Mining Sciences & Geomechanics Abstracts, Vol. 15, pp. 249-257.

D. J. Holcomb, 1988, "Crosshole Measurements of Velocity and Attenuation to Detect a Disturbed Rock Zone in Salt at the Waste Isolation Pilot Plant," Proceedings of the 29th US Symposium on Rock Mechanics, University of Minnesota, Minneapolis, June 23-25, pp. 633-640.

S. M. Howarth, E. W. Peterson, P. L. Lagus, K. Lie, S. J. Finley, and E. J. Nowak, 1991, "Interpretation of In-Situ Pressure and Flow Measurements of the Salado Formation at the Waste Isolation Pilot Plant", SPE paper 21840, submitted to the Society of Petroleum Engineers.

E. J. Nowak and D. F. McTigue, 1987, "Interim Results of Brine Transport Studies in the Waste Isolation Pilot Plant (WIPP)," Sandia National Laboratories Report SAND87-0880.

E. J. Nowak, D. F. McTigue, and R. Beraun, 1988, "Brine Inflow to WIPP Disposal Rooms: Data, Modeling, and Assessment," Sandia National Laboratories report SAND88-0112.

R. W. Ostensen, 1983, "Microcrack Permeability in Tight Gas Sands," Society of Petroleum Engineering Journal, Vol. 26, No. 6, pp. 919-927.

E. W. Peterson, P. L. Lagus, and K. Lie, 1987, "WIPP Horizon Free Field Fluid

Transport Characteristics,"Sandia National Laboratories report SAND87-7164 prepared by S-Cubed, LaJolla, CA.

G. J. Saulnier, Jr. and J. D. Avis, 1988, "Interpretation of Hydraulic Tests Conducted in the Waste-Handling Shaft at the Waste Isolation Pilot Plant (WIPP) Site," Sandia National Laboratories report SAND88-7001, prepared by Intera Technologies, Inc., Austin, TX.

J. C. Stormont, E. W. Peterson and P. L. Lagus, 1987, "Summary of and Observations about WIPP Facility Horizon Flow Measurements through 1986," Sandia National Laboratories report SAND87-0176.

J. C. Stormont, 1990a, "Summary of 1988 WIPP Facility Horizon Gas Flow Measurements," Sandia National Laboratories report SAND89-2497, Albuquerque, NM.

J. C. Stormont, 1990b, "Gas Permeability Changes in Rock Salt During Deformation," Ph.D. Dissertation, University of Arizona, Tucson.

USDOE, 1988, "Geotechnical Field Data and Analysis Report", July 1986 through June 1987, DOE/WIPP report 87-017, Carlsbad, NM.

J. B. Walsh, 1981, "Effect of Pore Pressure and Confining Pressure on Fracture Permeability," International Journal of Rock Mechanics and Mining Science & Geomechanics Abstracts, Vol. 18, pp. 429-435.

A Appendix A

A.1 Derivation of Governing Differential Equations

The mathematical expression which describes fluid flow through a porous medium is derived by combining the continuity equation, Darcy's law, and an equation of state. The continuity equation is derived by considering the mass balance over a representative elementary volume of the porous medium

$$\frac{\partial(\rho\phi)}{\partial t} = -\nabla \cdot (\rho v) \tag{A.1}$$

where ρ is the fluid density, v is the average fluid velocity, ϕ is the porosity of the porous medium, and t is time. From Walsh (1965), the time rate of change of the porosity can be expressed in terms of the compressibility of the solid material (C_s) and the bulk material (C)

$$\frac{\partial\phi}{\partial t} = [C - C_s(1+\phi)]\frac{\partial P}{\partial t} \tag{A.?}$$

The continuity equation therefore becomes

$$-\phi\frac{\partial\rho}{\partial t} - \rho C\frac{\partial P}{\partial t} + \rho C_s(1+\phi)\frac{\partial P}{\partial t} = \nabla \cdot (\rho v) \tag{A.3}$$

The average velocity of a fluid through a porous medium can be related to the pressure gradient (∇P) and the ratio of the permeability of the porous medium (k) to the viscosity of the fluid (μ) by means of Darcy's law

$$v = -\frac{k}{\mu}\nabla P \tag{A.4}$$

To complete the system of equations, an equation of state is introduced. For an ideal gas

$$\rho = \frac{PM}{RT} \tag{A.5}$$

where M is the molecular weight, R is the gas constant, and T is the temperature. Combining Equations A.3, A.4 and A.5 yields the governing differential equation for isothermal gas flow through a porous medium

$$\frac{\partial P^2}{\partial t} S = \nabla(\frac{k}{\mu} \nabla P^2) \tag{A.6}$$

where S is a storage coefficient

$$S = (C - C_s) + \phi(C_f - C_s) \tag{A.7}$$

where C_f is the compressibility of the fluid (in this case gas).

For brine flow, the variation of density with pressure is given by

$$\rho = \rho_o e^{C_b(P - P_o)} \tag{A.8}$$

where ρ_o is the initial density and C_b is the compressibility of brine. Combining Equations A.3, A.4, and A.8 yields the governing differential equation for isothermal brine flow through a porous medium

$$\frac{\partial P}{\partial t} S = \nabla(\frac{k}{\mu} \nabla P) \tag{A.9}$$

Note that the form of the differential equation for brine flow developed above is a special case of the general, three-dimensional poroelasticity theory and is equivalent to the model developed by Nowak and McTigue (1987) to model brine inflow to WIPP excavations. Poroelastic theory produces coupled constitutive equations for the total stress and the pore pressure. If we assume that the rock salt can be represented by an infinite medium with isotropic stresses, the constitutive equations can be uncoupled (Rice and Cleary, 1976) and the pore pressure can be solved for independently. If it is further assumed that the total mean stress in the rock remains constant and the volumetric strains are small, S becomes equivalent to the three-dimensional storage coefficient used in poroelasticity (van der Kamp and Gale, 1983) and the resulting poroelastic differential equation for the pore pressure is equivalent to Equation A.9.

A.2 Discussion of Assumptions

It is worthwhile to consider the assumptions inherent in the development of the governing differential equations for brine and gas flow (Equations A.6 and A.9).

1. Isothermal conditions - Although temperature measurements were only made of the brine and rock temperature in one borehole at 1.25 r, thermal effects are believed to be negligible for these measurements. The brine temperature measurement reveals that temperature changes during the initial, pre-excavation build-up period are less than 0.05 $^{\circ}C$. For a thermal expansivity of $3\text{x}10^{-4}$ K^{-1} and a test interval compressibility of $2\text{x}10^{-9} Pa^{-1}$, the thermally induced pressure change is less than 10 kPa. We expect the other test intervals to equilibrate with the formation during the relatively long duration shut-in period and have similar temperature histories. For a similar temperature change in a gas-filled test interval, the corresponding pressure change is less than 1 kPa. Thus, thermal effects are not significant for the long duration shut-in tests.

Thermal effects during the post-excavation injection tests are also believed to be negligible. For gas flow tests similar to those conducted during the injection tests in the gas-filled test intervals, Stormont (1990a) found no significant temperature effects during both constant-pressure and shut-in tests. We also expect the thermal effects during the brine-injection tests to be small. For example, even if the injection test results in a temperature change of 5 $^{\circ}C$, the injected volume of brine and consequently the interpreted permeability is altered by less than 10%.

2. Laminar flow - When streamlines become distorted, Darcy's law breaks down (Dullien, 1979). The lowest critical Reynolds number above which Darcy's law is no longervalid is 1 to 10 (Bear, 1979). The Reynolds number is calculated as (Bear, 1979)

$$Re = \frac{qd}{\nu} \tag{A.10}$$

where q is the specific discharge or flux, d is some representative length of the porous medium (often taken as the grain size), and ν is the kinematic viscosity of the fluid.

The largest Reynolds numbers developed during the constant gas and brine injection tests at 1.25 r. For brine, the maximum flux was about 10^{-9} m/sec and the corresponding Reynolds number was about 10^{-4}. For gas flow, the maximum flux was about $1\text{x}10^{-4}$ m/sec at standard conditions and the corresponding Reynolds number is about $3\text{x}10^{-3}$. Clearly, the flow was not sufficient to invalidate Darcy's law.

3. The flow is radial - The flow geometry assumed for our analysis is radial flow to or from the test interval. Radial flow may be the most realistic for a horizontally bedded

formation if the different layers have different hydrologic properties. Recent hydrologic testing at the WIPP horizon strongly suggests that the formation is heterogeneous, and different layers (even amongst various halite layers) may possess quite different hydrologic properties (Howarth et al. , 1991; Beauheim et al., 1991).

However, if the test interval layer and the adjacent rock have similar properties, then cylindrical flow may be a more appropriate assumption. In this case, the validity of radial flow is a function of the length-to-diameter ratio of the test interval (Marinelli, 1984). For a similar length-to-diameter ratio as that employed in these tests, Stormont (1990a) found that the radial flow geometry assumption introduced a maximum error of 25%.

4. The flowing fluid is a single, nonreactive phase - There is uncertainity both with b ne flow and gas flow in regard to single-phase flow. It is not obvious that the flow induced toward a borehole during a build-up test is simply brine flow. The intergranular porosity contains some gas, either free or dissolved in the brine. Gas production into some some sealed boreholes has been detected (Peterson et al., 1985; Borns and Stormont, 1989) and gas has been observed bubbling up through the brine in some holes (Lappin et al., 1989). Chemical analyses revealed that the gas is principally nitrogen, and its origin is presumably from the original deposition of the evaporite deposit (Niou et al., 1988). It is not known if there is free gas in the formation at the equilibrium pore pressure, or if it only exsolves as the brine pressure is reduced.

Brine is also reactive with the host rock. The solubility of sodium chloride in water increases with pressure. Changes in the brine pressure due to flow or changes in the total stress applied to the matrix could dissolve or precipitate salt along the flow path, changing the permeability. Baes et al. (1983) observed permeability reductions with time due to this phenomenon in the laboratory. Because of the very small dimensions of the flow paths, Lappin et al. (1989) suggested that interaction between pore brine and the solid surfaces can result in non-Darcy flow.

When gas is injected into the formation, the question of whether it the only fluid which flows or if induce two-phase (gas and brine) flow arises. Pre-existing brine in the flow path can greatly affect the resulting gas flow and consequently the calculated permeability. It is unlikely that the injected gas will displace pre-existing brine because of the capillary forces that exist in intact rock salt. Stormont et al. (1987) argued that injected gas should not displace pore brine unless the pore sizes are much larger than that typically assumed for intact rock salt or the rock tested was not completely brine-saturated. Because there are no data on brine displacement from injected gas in brine-saturated rock salt, it will be assumed that only the injected gas is flowing. The implication of this assumption is that if the formation was originally fully brine-saturated, the gas will be flowing through porosity which has been created or has dilated subsequent to the excavation process. The dissolution of nitrogen into pore

brine is believed to be small and not accounted for.

5. Gas is ideal - For an ideal gas, the viscosity is independent of pressure and the real gas correction factor (or compressibility factor) equals unity in the equation of state, allowing simplifications in the development of the governing differential equation. The gas used for all of the gas flow test was nitrogen - can it be considered ideal?

The use of reduced state variables permits the deviation from ideal behavior to be assessed. The reduced pressure, P_r, is given by

$$P_r = \frac{P}{P_c} \tag{A.11}$$

and the reduced temperature, T_r, is given by

$$T_r = \frac{T}{T_c} \tag{A.12}$$

where P is the pressure, P_c is the critical pressure, T is the temperature, and T_c is the critical temperature. The behavior of all gases is the same with respect to the reduced state variables. The critical pressure and temperature for nitrogen were obtained from The Handbook of Chemistry and Physics (Weast, 1978, p. F-90). At extreme values of the reduced pressure and temperature applicable for the gas flow tests described here, the viscosity change from standard conditions is <1% (Katz et al., 1959, Figure 4-102 and Figure 4-103, p. 173) and the real gas correction factor is between 0.99 and 1.00 (Katz et al., 1959, Table A-2, p. 710). Therefore, the assumption that the injected fluid is an ideal gas is justified at these test conditions.

In all of the analyses, we further simplified our model by assuming that all hydraulic properties (permeability, porosity, and storage) are homogeneous. There are many reasons why this assumption may not be applicable, but we lack better information in this area. Possible reasons the assumption of homogeneity may not be valid include:

- Damage - Regions of damage may surround the monitoring borehole in the form of microcracks developing and dilating along grain boundaries (Stormont, 1990b). Damage increases the permeability, porosity, and bulk compressibility (and therefore storage) of the formation. Stormont (1990a) found that many gas flow tests were simulated better with a model which incorporated a local DRZ surrounding the test borehole.

- Changes in effective stress - The pore structure, and hence permeability and porosity, of geologic materials are assumed to be controlled by the effective stress σ_e, which is defined as

$$\sigma_e = \sigma - \delta a u \tag{A.13}$$

where σ is the total stress, δ is the Kronecker delta, u is the hydrostatic (pore) pressure, and a is a parameter that reflects the relative influence of the hydrostatic pressure. Because both the total stress and the fluid pressure are altered in the vicinity of an excavation, the effective stress surrounding both the large-diameter borehole and the monitoring boreholes will not be constant. Therefore, the permeability and porosity may be altered.

Skempton (1961) showed that a can be expressed as

$$a = 1 - \frac{C_s}{C} \tag{A.14}$$

where C_s and C are the compressibilities of the solid and bulk material, respectively. For a material with low porosity, the bulk compressibility approaches that of the solid, a tends toward zero and the effective stress is essentially the total stress. For the compressibilities associated with intact or undisturbed rock salt (e.g., Nowak et al., 1988), a is about 0.1. In a DRZ (whether globally associated with the large-diameter borehole or locally associated with the monitoring borehole), the effective stress law may have a greater significance. The development of microcracks in the DRZ will render the rock more compressible (Budiansky and O'Connell, 1976), the value of a will increase, and the fluid pressure will have a greater influence on the effective stress. Thus, the effective stress law for rock salt is a function of the degree of damage it has sustained.

- Pore pressure - Permeability may be a function of the pore pressure beyond effective stress effects. Because sodium chloride solubility in brine is a function of pressure, the permeability may be altered by dissolution and/or precipitation along the flow paths.

- Gas slip - When the mean free path of the gas molecule approaches the size of the flow path, substantial interaction between the gas molecule and the flow path surface will occur. This interaction, referred to as gas slip, will result in a component of flow in addition to that due to a pressure gradient (Darcy flow). Because the mean free path of the gas molecule is a function of its pressure, the magnitude of this effect and consequently the interpreted permeability is a

function of the pore pressure and the specific gas properties. The apparent or measured gas permeability can be up to an order of magnitude greater than the intrinsic or liquid permeability. A correction for gas slip can be developed from laboratory gas permeability tests. Sutherland and Cave (1980) and Peach et al. (1987) interpret their laboratory data as indicating there is no significant gas slip correction required for rock salt for permeabilities of about 10^{-19} m^2. Stormont (1990b) found that the sensitivity of the pore structure of rock salt to changes in pore and external confining stresses makes determination of a gas slip correction difficult unless the permeability is greater than 10^{-16} m^2. Thus, while gas slip effects may be inherent in the data, there is no clear information or indication regarding a relevant correction.

- Fluid compressibiltiy - As the pore fluid moves toward a lower pressure such as a drift or borehole, dissolved gas may exsolve and dramatically increase the compressibility and consequently the hydraulic storage term.

- Local variations in rock properties due to compositional or depositional differences - Recent experimental evidence of the heterogeneity of the formation suggests that even within the same layer, hydrologic properties may vary spatially.

A.3 Initial and Boundary Conditions

The initial condition is a known (not necessarily constant) pressure field (P) in the rock

$$P = P^o(r) \qquad a < r < \infty, t = 0 \tag{A.15}$$

At the outer boundary, that is, far from the test interval, the pressure is assumed to be constant with time. The boundary condition at the outer boundary for both brine and gas flow is

$$\frac{\partial P}{\partial t} = 0 \qquad r = \infty, t \geq 0 \tag{A.16}$$

There are five boundary conditions relevant to the test interval:

- brine flow to or from a brine-filled, shut-in test interval
- brine flow to or from a partially gas-filled, shut-in test interval
- constant-pressure brine injection
- constant-pressure gas injection
- pressure-pulse gas injection

A.3.1 Shut-in test interval with brine inflow or outflow

The flowrate at the borehole wall due to brine inflow or outflow is

$$\frac{\partial V}{\partial t} = -\frac{k}{\mu} A(\nabla P) \tag{A.17}$$

where V is borehole fluid volume, k and μ are the permeability and viscosity of the formation at the borehole wall, and A is the surface area of the test interval. For a completely brine-filled borehole, the pressure change within the borehole due to the brine flow is

$$\frac{\partial P}{\partial t} = \frac{1}{C_b V_b} \frac{\partial V}{\partial t} \tag{A.18}$$

where C_b is the compressibility of the test interval brine. Combining 17 and 18 yields

$$\frac{\partial P}{\partial t} = -\frac{k}{\mu} \frac{A}{V_b C_b} (\nabla P) \qquad r = a, t > 0 \tag{A.19}$$

Next consider a test interval which contains some gas, but the formation permits only brine flow. That is, the formation has no permeability to gas. The test interval fluid compressibility is dominated by the gas compressibility, $C_g = P^{-1}$, so the change in volume of the test interval fluids in response to brine inflow or outflow is given as

$$\frac{\partial V}{\partial t} = \frac{V_g}{P} \frac{\partial P}{\partial t} \tag{A.20}$$

where V_g is the volume of gas in the test interval.

Combining 17 and 20 yields

$$\frac{\partial P}{\partial t} = -\frac{k}{\mu} \frac{A}{V_g} P \nabla P \qquad r = a, t > 0 \tag{A.21}$$

The time-dependent creep of rock salt may result in the closure of test intervals, which in turn will induce pressure changes in shut-in test intervals. The radial closure rate of the test interval is assumed to be

$$\frac{\partial r}{\partial t} = -\alpha r (\sigma - P)^n \tag{A.22}$$

where σ is the far-field stress, P is the test interval pressure, n is the stress exponent, and α is an empirical constant. This expression is a modified form of a closed-form solution of Chabannes (1982) for secondary creep closure of an infinitely long cylinder in an infinite medium. The stress exponent for secondary creep of WIPP rock salt has been found to be near 5 (e.g., Munson et al., 1989). Because the closure rate is a function of the test interval pressure, the closure rate will be time-dependent. The

value of α can be selected to provide any open hole closure rate desired, such as a field-measured value.

For a brine-filled test interval, the rate of pressure change is

$$\frac{\partial P}{\partial t} = \frac{\pi L}{C_b V_b}[(-2\alpha a^2(\sigma - P)^n) + (-\alpha a(\sigma - P)^n)^2] \tag{A.23}$$

For a test interval which contains gas, the rate of pressure change due to test interval closure is

$$\frac{\partial P}{\partial t} = \frac{\pi L P}{V_g}[(-2\alpha a^2(\sigma - P)^n) + (-\alpha a(\sigma - P)^n)^2] \tag{A.24}$$

The combined effect of brine inflow/outflow and test interval closure is given by combining Equations A.19 and A.23 for a brine-filled test interval, and combining Equations A.21 and A.24 for a test interval which contains some gas.

A.3.2 Constant-pressure brine and gas injection

During constant-pressure brine and gas-injection tests, the test interval pressure is maintained at a constant-pressure by means of a regulated external reservoir. The boundary condition for these tests is given by

$$\frac{\partial P}{\partial t} = 0 \qquad r = a, t > 0 \tag{A.25}$$

The principal advantage of this type of test is that the compressibility of the test interval is not a factor in the interpreted formation properties (Doe et al., 1989).

A.3.3 Pressure-pulse gas injection

In these tests, gas is flowing from the test interval into the formation. The rate of pressure change in the test interval is given by

$$\frac{\partial P}{\partial t} = \frac{P}{V_g}\frac{\partial V}{\partial t} \tag{A.26}$$

Combined with the test interval flux, the resulting boundary condition is

$$\frac{\partial P}{\partial t} = \frac{k_g}{\mu_g}\frac{A}{V_g}P\nabla P \qquad r = a, t > 0 \tag{A.27}$$

Here, gas permeability and viscosity is explicitly denoted by the subscript g.

The effect of closure of the test interval can be added to this boundary condition as desired. All of the boundary conditions for gas can be expressed in terms of P^2 instead of P.

A.4 Numerical Simulation of Fluid Flow in a Porous Medium

A finite difference solution to Equations A.6 and A.9 was developed to simulate the measurements of gas flow. The finite difference method involves discretization of the domain into a number of finite lengths connected by nodes. Approximations to derivatives of functions are made at nodes, substituted into the differential equation, and the resulting system of equations is solved. In essence, the governing partial differential equation is approximated by a series of ordinary differential equations. The numerical solution follows from that of Nowak and McTigue (1987).

For radial gas flow, Equation A.6 can be written as

$$\frac{\partial P^2}{\partial t} = S^{-1}\frac{1}{r}\frac{\partial}{\partial r}[Kr\frac{\partial P^2}{\partial r}] \tag{A.28}$$

where K is $\frac{k}{\mu}$. A central difference approximation to the spatial derivative of the term in brackets gives

$$\frac{dP_i^2}{dt} = S_i^{-1}\frac{1}{r_i}[\frac{r_{i+1/2}}{\Delta}K_{i+1/2}\frac{\partial P_{i+1/2}^2}{\partial r} - \frac{r_{i-1/2}}{\Delta}K_{i-1/2}\frac{\partial P_{i-1/2}^2}{\partial r}] \tag{A.29}$$

where i refers to the node number and Δ is the distance between nodes i and $i+1$. The remaining spatial derivatives can then be approximated by a central difference approximation, yielding

$$\frac{dP_i^2}{dt} = S_i^{-1}\frac{1}{r_i}[\frac{r_{i+1/2}}{\Delta^2}K_{i+1/2}(P_{i+1}^2 - P_i^2) - \frac{r_{i-1/2}}{\Delta^2}K_{i-1/2}(P_i^2 - P_{i-1}^2)] \tag{A.30}$$

K is calculated at the midpoint between i and $i+1$, S_i^{-1} is calculated at node i. Both S^{-1} and K can be a function of position, pressure, or time. The numerical approximation for radial brine flow is equivalent to Equation A.28 with P^2 replaced by P.

The resulting system of equations is solved using a backward differencing solver subroutine (available from Sandia National Laboratories' technical library) which is unconditionally stable and optimizes the time step for accuracy (Shampine and Watts, 1979). The value of the independent variable (P or P^2) is calculated and given at discrete times on the way to the final time. Other quantities such as the flowrate and flux can be calculated as desired.

The discretization of the domain for the simulation of the in situ measurements should consider a number of factors. First, the number of nodes should be minimized in order to limit the size of the system of equations which is to be solved. Next, the location of the remote boundary (or last node) should be sufficiently far from the borehole so Equation A.16 remains valid at all times. Also, calculated pressure gradients in the vicinity of the borehole will be large, and the accuracy of the approximation is improved if discretization is fine in this region. Finally, the discretization should be suitable for wide ranges of permeabilities, pressures, and times. In order to best accomodate these factors, the following coordinate transformation given by Nowak and McTigue (1987) was employed

$$x = 1 - e^{-\xi(\frac{r}{a}-1)} \tag{A.31}$$

where x is the transformed coordinate, r is the radial coordinate, a is the borehole radius, and ξ is the stretch factor. The transformed coordinate varies from $x = 0$ at the borehole wall to $x = 1$ at an infinite radius. With this transformation, nodes can be concentrated in the vicinity of the borehole while the remote boundary is at infinity.

A.5 Verification

In order to ensure the accuracy of the code, the numerical solution was compared with the analytical solution of Cooper et al. (1967) as given by Bredehoeft and Papadopulos (1980) for the borehole pressure history during a water pressure-pulse test. The numerical solution was found to be essentially identical for simulations with 100 to 200 nodes and stretch factors of 0.1 to 0.01. The numerical results and analytical solutions are shown to compare very well (Figure A.1).

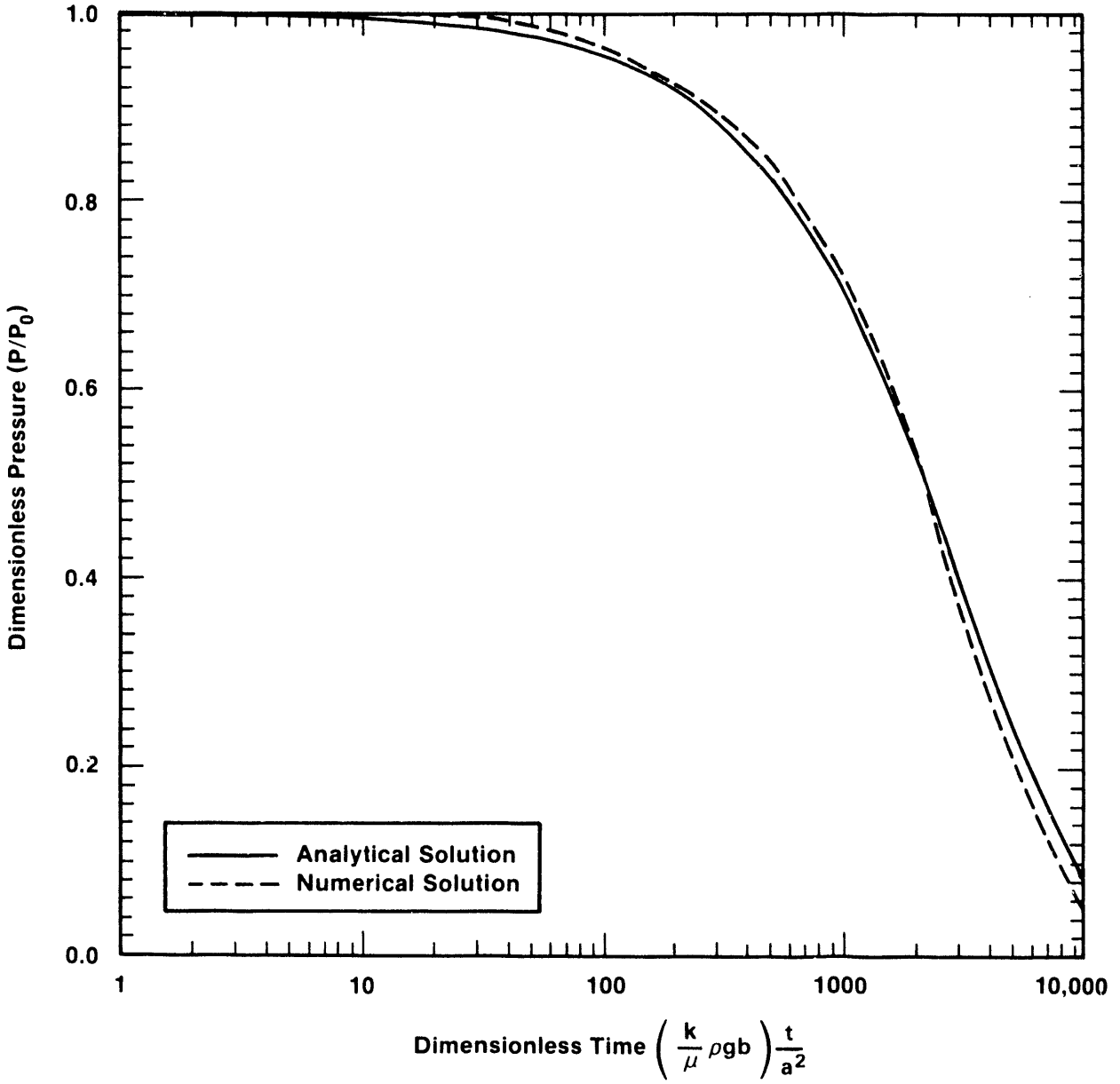

Figure A.1: Comparison of analytical and numerical solutions for slug test using water; ρ is density of fluid, g is gravitational constant, b is length of test interval. Other terms are defined in text.

A.6 Material properties and test interval dimensions

The material properties used in the model simulations are given in the following table.

Table A.I

Property	Value	Source
Effective halite compressibility	4.83×10^{-11} Pa^{-1}	Nowak et al., 1988
Solid halite compressibility	4.25×10^{-11} Pa^{-1}	Nowak et al., 1988
Brine viscosity	1.6×10^{-3} Pa-sec	Nowak et al., 1988
Brine compressibility	5×10^{-10} Pa^{-1}	Nowak et al., 1988
Nitrogen viscosity	1.8×10^{-5} Pa-sec	Weast, 1979
Nitrogen compressibility	P^{-1} Pa^{-1}	-

The test interval dimensions, as derived from measurements of borehole diameter and the position of the packer system in the borehole, are compiled in the following table.

Table A.II

Borehole Number	Diameter (cm)	Test Interval Volume (cc)	Test Interval Length (cm)
50	4.72	653	67.0
51	4.72	631	66.0
52	4.72	631	66.0
53	4.72	578	63.8
54	4.72	634	66.2
55	4.71	564	63.5
56	4.72	631	66.0
57	4.78	648	64.8
58	4.72	570	63.5
59	4.70	619	65.0
60	4.67	562	64.1
61	4.75	594	64.0

A.7 References

C. F. Baes, Jr., L. O. Gilpatrick, F. G. Kitts, H. R. Bronstein and A. J. Shor, 1983, "The Effect of Water in Salt Repositories: Final Report", Oak Ridge National Laboratory report ORNL-5950, Oak Ridge, TN.

J. Bear, 1979, Hydraulics of Groundwater, McGraw-Hill Book Company, New York.

R. L. Beauheim, G. J. Saulnier, Jr. and J. D. Avis, 1991, "Interpretation of Brine-Permeability Tests of the Salado Formation at the Waste Isolation Pilot Plant Site: First Interim Report," Sandia National Laboratories report in preparation.

D. J. Borns and J. C. Stormont, 1989, "The Delineation of the Disturbed Rock Zone Surrounding Excavations in Salt," Rock Mechanics as a Guide to Efficient Utilization of Natural Resources, Proceedings of the 30th US Symposium on Rock Mechanics, West Virginia University, Morgantown, June 19-22, A. A. Balkema, Rotterdam, pp. 353-360.

J. D. Bredehoeft and S. S. Papadopulos, 1980, " A Method for Determining the Hydraulic Properties of Tight Formations", Water Resources Research, Vol. 16, No. 1, pp. 233-238.

B. Budiansky and R. J. O'Connell, 1976, "Elastic Moduli of a Cracked Solid," International Journal of Solids and Structures, Vol. 12, pp. 81-97.

C. R. Chabannes, 1982, "An Evaluation of the Time-Dependent Behavior of Solution-Mined Cavities in Salt for the Storage of Natural Gas", M.Sc. Thesis, Pennsylvania State University, State College, PA.

H. H. Cooper, Jr., J. D. Bredehoeft and I. S. Papadopulos, 1967, "Response of a Finite Diameter Well to an Instantaneous Charge of Water," Water Resources Research, Vol. 3, No. 1, pp. 461-467.

T. W. Doe, J. Osnes, M. Kendrick, J. Geier, and S. Warner, 1989, "Design of Borehole Testing Programs for Waste Disposal Sites in Crystalline Rocks," Proceedings of the Sixth International Congress on Rock Mechanics, Montreal, 1987, A. A. Balkema, Rotterdam, Vol. 3, pp.1377-1398.

F. A. L. Dullien, 1979, Porous Media: Fluid Transport and Pore Structure, Academic Press, New York.

S. M. Howarth, E. W. Peterson, P. L. Lagus, K. Lie, S. J. Finley, and E. J. Nowak, 1991, "Interpretation of In-Situ Pressure and Flow Measurements of the Salado For-

mation at the Waste Isolation Pilot Plant", SPE paper 21840, submitted to the Society of Petroleum Engineers.

D. L. Katz, D. Cornell, R. Kobayashi, F. H. Poettmann, J. A. Vary, J. R. Elenbaas, and C. F. Weinaug, 1959, Handbook of Natural Gas Engineering, McGraw-Hill Book Company.

A. R. Lappin, R. L. Hunter, Editors, D. P. Garber, P. B. Davies, Associate Editors, 1989, "System Analysis, Long-Term Radionuclide Transport, and Dose Assessments, Waste Isolation Pilot Plant (WIPP), Southeastern New Mexico; March, 1989," Sandia National Laboratories report SAND89-0462, Albuquerque, NM.

F. Marinelli, 1984, "Analysis of Constant Head Injection Tests in Single, Partially Penetrating Boreholes," M.Sc. Thesis, University of Arizona, Tucson, AZ.

D. E. Munson, A. F. Fossum and P. E. Senseny, 1989, "Advances in Resolution of Discrepancies Between Predicted and Measured In Situ WIPP Room Closure," Sandia National Laboratories report SAND88-2948, Albuquerque, NM.

S. Niou, W. W. Irwin and D. E. Deal, 1989, "Migration of Brine and Nitrogen in Creeping Salt," Waste Management 89 Symposium, Tuscon, AZ, February 26-March 2, Vol. 1, pp. 329-335.

E. J. Nowak and D. F. McTigue, 1987, "Interim Results of Brine Transport Studies in the Waste Isolation Pilot Plant (WIPP)," Sandia National Laboratories Report SAND87-0880.

E. J. Nowak, D. F. McTigue, and R. Beraun, 1988, "Brine Inflow to WIPP Disposal Rooms: Data, Modeling, and Assessment," Sandia National Laboratories report SAND88-0112.

C. J. Peach, C. J. Spiers, A. J. Tankink, and H. J. Zwart, 1987, "Fluid and Ionic Transport Properties of Deformed Salt Rock," Commission of the European Communities report EUR10926, Luxembourg.

E. W. Peterson, P. L. Lagus, J. Brown, and K. Lie, 1985, "WIPP Horizon In Situ Permeability Measurements Final Report,"Sandia National Laboratories report SAND85-7166 prepared by S-Cubed, LaJolla, CA.

J. R. Rice and M. P. Cleary, 1976, "Some Basic Stress-Diffusion Solutions for Fluid-Saturated Elastic Porous Media with Compressible Constituents," Reviews of Geophysics and Space Physics, Vol. 14, pp. 227-241.

L. F. Shampine and H. A. Watts, 1979, "DEPAC - Design of a User Oriented Package of ODE Solvers," Sandia National Laboratories report SAND79-2374, Albuquerque,

NM.

A. W. Skempton, 1961, "Effective Stress in Soils, Concrete and Rock," Pore Pressure and Suction in Soils, Butterworth, London, pp. 4-16.

J. C. Stormont, E. W. Peterson and P. L. Lagus, 1987, "Summary of and Observations about WIPP Facility Horizon Flow Measurements through 1986," Sandia National Laboratories report SAND87-0176.

J. C. Stormont, 1990a, "Summary of 1988 WIPP Facility Horizon Gas Flow Measurements," Sandia National Laboratories report SAND89-2497, Albuquerque, NM.

J. C. Stormont, 1990b, "Gas Permeability Changes in Rock Salt During Deformation," Ph.D. Dissertation, University of Arizona, Tucson.

H. J. Sutherland and S. P. Cave, 1980, "Argon-gas Permeability of New Mexico Rock Salt Under Hydrostatic Compression," International Journal of Rock Mechanics and Mining Sciences & Geomechanics Abstracts, Vol. 17, pp. 281-288.

G. van der Kamp and J. E. Gale, 1983, "Theory of Earth Tide and Barometric Effects In Porous Formations With Compressible Grains," Water Resources Research, Vol. 19, No. 2, pp. 538-544.

J. B. Walsh, 1965, "The Effect of Cracks on the Compressibility of Rock," Journal of Geophysical Research, Vol. 70, No. 2, p. 381-389.

R. C. Weast, editor, 1979, CRC Handbook of Chemistry and Physics, 59th Edition, CRC Press, West Palm Beach, FL.

Federal Agencies

U.S. Department of Energy, (5)
Office of Civilian Radioactive Waste Management
Attn: Deputy Director, RW-2
Associate Director, RW-10
Office of Program Administration and Resources Management
Associate Director, RW-20
Office of Facilities Siting and Development
Associate Director, RW-30
Office of Systems Integration and Regulations
Associate Director, RW-40
Office of External Relations and Policy
Forrestal Building
Washington, DC 20585

U.S. Department of Energy (3)
Albuquerque Operations Office
Attn: J.E. Bickel
R. Marquez, Director
Public Affairs Division
P.O. Box 5400
Albuquerque, NM 87185

U.S. Department of Energy
Attn: National Atomic Museum Library
Albuquerque Operations Office
P.O. Box 5400
Albuquerque, NM 87185

U.S. Department of Energy (4)
WIPP Project Office (Carlsbad)
Attn: V. Daub
J.A. Mewhinney
P.O. Box 3090
Carlsbad, NM 88221

U.S. Department of Energy
Research & Waste Management Division
Attn: Director
P.O. Box E
Oak Ridge, TN 37831

U.S. Department of Energy
Waste Management Division
Attn: R.F. Guercia
P.O. Box 550
Richland, WA 99352

U.S. Department of Energy
Attn: E. Young
Room E-178
GAO/RCED/GTN
Washington, DC 20545

U.S. Department of Energy (6)
Office of Environmental Restoration and Waste Management
Attn: J. Lytl , EM30
M. Frei, EM-34 (3)
M. Duff, EM-34
C. Frank, EM-50
Washington, DC 20585

U.S. Department of Energy (3)
Office of Environment, Safety and Health
Attn: R. Pelletier, EH-231
K. Taimi, EH-232
C. Borgstrom, EH-25
Washington, DC 20585

U.S. Department of Energy (2)
Idaho Operations Office
Fuel Processing and Waste Management Division
785 DOE Place
Idaho Falls, ID 83402

U.S. Department of Energy
Savannah River Operations Office
Defense Waste Processing Facility Project Office
Attn: W.D. Pearson
P.O. Box A
Aiken, SC 29802

U.S. Environmental Protection Agency (2)
Attn: R. Clark
Office of Radiation Programs (ANR-460)
Washington, DC 20460

U.S. Geological Survey
Branch of Regional Geology
Attn: R. Snyder
MS913, Box 25046
Denver Federal Center
Denver, CO 80225

U.S. Geological Survey
Conservation Division
Attn: W. Melton
P.O. Box 1857
Roswell, NM 88201

U.S. Geological Survey (2)
Water Resources Division
Attn: K. Peter
Suite 200
4501 Indian School, NE
Albuquerque, NM 87110

U.S. Nuclear Regulatory Commission (4)
Attn: J. Bunting, HLEN 4H3 OWFN
R. Ballard, HLGP 4H3 OWFN
J. Philip
NRC Library
Mail Stop 623SS
Washington, DC 20555

Boards

Defense Nuclear Facilities Safety Board
Attn: D. Winters
Suite 700
625 Indiana Ave., NW
Washington, DC 20004

U.S. Department of Energy
Advisory Committee on Nuclear
Facility Safety
Attn: M.E. Langston, AC21
Washington, DC 20585

Nuclear Waste Technical Review Board (2)
Attn: D.A. Deere
S.J.S. Parry
Suite 910
1100 Wilson Blvd.
Arlington, VA 22209-2297

Richard Major
Advisory Committee on Nuclear Waste
Nuclear Regulatory Commission
7920 Norfolk Avenue
Bethesda, MD 20814

State Agencies

Environmental Evaluation Group (3)
Attn: Library
Suite F-2
7007 Wyoming, NE
Albuquerque, NM 87109

New Mexico Bureau of Mines
and Mineral Resources (2)
Attn: F.E. Kottolowski, Director
J. Hawley
Socorro, NM 87801

NM Department of Energy & Minerals
Attn: Librarian
2040 S. Pacheco
Santa Fe, NM 87505

NM Environmental Improvement Division
Attn: Deputy Director
1190 St. Francis Drive
Santa Fe, NM 87503

Laboratories/Corporations

Battelle Pacific Northwest Laboratories
(5)
Attn: D.J. Bradley, K6-24
J. Relyea, H4-54
R.E. Westerman, P8-37
H.C. Burkholder, P7-41
L. Pederson, K6-47
Battelle Boulevard
Richland, WA 99352

Savannah River Laboratory (6)
Attn: N. Bibler
E.L. Albenisius
M.J. Plodinec
G.G. Wicks
C. Jantzen
J.A. Stone
Aiken, SC 29801

George Dymmel
SAIC
101 Convention Center Dr.
Las Vegas, NV 89109

INTERA Technologies, Inc. (4)
Attn: G.E. Grisak
J.F. Pickens
A. Haug
A.M. LaVenue
Suite #300
6850 Austin Center Blvd.
Austin, TX 78731

INTERA Technologies, Inc.
Attn: W. Stensrud
P.O. Box 2123
Carlsbad, NM 88221

IT Corporation (2)
Attn: R.F. McKinney
J. Myers
Regional Office - Suite 700
5301 Central Avenue, NE
Albuquerque, NM 87108

IT Corporation (2)
Attn: D.E. Deal
P.O. Box 2078
Carlsbad, NM 88221

Los Alamos Scientific Laboratory
Attn: B. Erdal, CNC-11
Los Alamos, NM 87545

RE/SPEC, Inc. (4)
Attn: W. Coons
Suite 300
4775 Indian School, NE
Albuquerque NM 87110-3927

RE/SPEC, Inc. (7)
Attn: A.F. Fossum
G. Callahan
T. Pfeifle
J.L. Ratigan
P.O. Box 725
Rapid City, SD 57709

Center for Nuclear Waste
Regulatory Analysis (4)
Attn: P.K. Nair
Southwest Research Institute
6220 Culebra Road
San Antonio, TX 78228-0510

Science Applications
International Corporation
Attn: H.R. Pratt,
Senior Vice President
10260 Campus Point Drive
San Diego, CA 92121

Science Applications
International Corporation
Attn: M.B. Gross
Asst. Vice President
Suite 1250
160 Spear Street
San Francisco, CA 94105

Systems, Science, and Software (2)
Attn: E. Peterson
Box 1620
La Jolla, CA 92038

Tech Reps., Inc.
Attn: E. Lorusso
5000 Marble, NE
Albuquerque, NM 87110

Westinghouse Electric Corporation (7)
Attn: Library
L. Trego
W.P. Poirer
W.R. Chiquelin
V.F. Likar
D.J. Moak
R.F. Kehrman
P.O. Box 2078
Carlsbad, NM 88221

Weston Corporation
Attn: D. Lechel
Suite 1000
5301 Central Avenue, NE
Albuquerque, NM 87108

Universities

University of Arizona
Attn: J.G. McCray
Department of Nuclear Engineering
Tucson, AZ 85721

University of New Mexico
Geology Department
Attn: Library
Albuquerque, NM 87131

Pennsylvania State University
Materials Research Laboratory
Attn: D. Roy
University Park, PA 16802

Texas A&M University
Center of Tectonophysics
College Station, TX 77840

University of Washington
Attn: G.R. Heath
College of Ocean
and Fishery Sciences
Seattle, WA 98195

Individuals

D.W. Powers
Star Route Box 87
Anthony, TX 79821

Libraries

Thomas Brannigan Library
Attn: D. Dresp, Head Librarian
106 W. Hadley St.
Las Cruces, NM 88001

Hobbs Public Library
Attn: M. Lewis, Librarian
509 N. Ship Street
Hobbs, NM 88248

New Mexico State Library
Attn: I. Vollenhofer
P.O. Box 1629
Santa Fe, NM 87503

New Mexico Tech
Martin Speere Memorial Library
Campus Street
Socorro, NM 87810

Pannell Library
Attn: R. Hill
New Mexico Junior College
Lovington Highway
Hobbs, NM 88240

WIPP Public Reading Room
Attn: Director
Carlsbad Public Library
101 S. Halagueno St.
Carlsbad, NM 88220

Government Publications Department
General Library
University of New Mexico
Albuquerque, NM 87131

The Secretary's Blue Ribbon Panel on WIPP

Dr. Thomas Bahr
New Mexico Water Resources Institute
New Mexico State University
Box 3167
Las Cruces, NM 88003-3167

Mr. Leonard Slosky
Slosky and Associates
Suite 1400
Bank Western Tower
1675 Tower
Denver, CO 80202

Mr. Newal Squyres
Holland & Hart
P.O. Box 2527
Boise, ID 83701

Dr. Arthur Kubo
Vice President
BDM International, Inc.
7915 Jones Branch Drive
McLean, VA 22102

Mr. Robert Bishop
Nuclear Management Resources Council
Suite 300
1776 I Street, NW
Washington, DC 20006-2496

National Academy of Sciences, WIPP Panel

Dr. Charles Fairhurst, Chairman
Department of Civil and
Mineral Engineering
University of Minnesota
500 Pillsbury Dr. SE
Minneapolis, MN 55455-0220

Howard Adler
Oak Ridge Associated Universities
Medical Sciences Division
P.O. Box 117
Oak Ridge, TN 37831-0117

Dr. John O. Blomeke
3833 Sandy Shore Drive
Lenoir City, TN 37771

Dr. John D. Bredehoeft
Western Region Hydrologist
Water Resources Division
U.S. Geological Su y (M/S 439)
345 Middlefield Road
Menlo Park, CA 94025

Dr. Fred M. Ernsberger
250 Old Mill Road
Pittsburgh, PA 15238

Dr. Rodney C. Ewing
Department of Geology
University of New Mexico
Albuquerque, NM 87131

B. John Garrick
Pickard, Lowe & Garrick, Inc.
Suite 400
4590 MacArthur Blvd.
Newport Beach, CA 92660-2027

Leonard F. Konikow
U.S. Geological Survey
431 National Center
Reston, VA 22092

Jeremiah O'Driscoll
Jody Incorporated
505 Valley Hill Drive
Atlanta, GA 30350

Dr. Christopher G. Whipple
Clement International
Suite 1380
160 Spear Street
San Francisco, CA 94105

Dr. Peter B. Myers
National Academy of Sciences
Committee on Radioactive
Waste Management
2101 Constitution Avenue
Washington, DC 20418

Dr. Geraldine Grube
Board on Radioactive
Waste Management
GF456
2101 Constitution Avenue
Washington, DC 20418

Foreign Addresses

Studiecentrum Voor Kernenergie
Centre D'Energie Nucleaire
Attn: Mr. A. Bonne
SCK/CEN
Boeretang 200
B-2400 Mol
BELGIUM

Atomic Energy of Canada, Ltd. (2)
Whiteshell Research Estab.
Attn: Peter Haywood
John Tait
Pinewa, Manitoba, CANADA
ROE 1LO

Dr. D. K. Mukerjee
Ontario Hydro Research Lab
800 Kipling Avenue
Toronto, Ontario, CANADA
M8Z 5S4

Mr. Francois Chenevier, Director (2)
ANDRA
Route du Panorama Robert Schumann
B.P.38
92266 Fontenay-aux-Roses Cedex
FRANCE

Mr. Jean-Pierre Olivier
OECD Nuclear Energy Agency
Division of Radiation Protection
and Waste Management
38, Boulevard Suchet
75016 Paris, FRANCE

Claude Sombret
Centre D'Etudes Nucleaires
De La Vallee Rhone
CEN/VALRHO
S.D.H.A. BP 171
30205 Bagnols-Sur-Ceze
FRANCE

Bundesministerium fur Forschung und
Technologie
Postfach 200 706
5300 Bonn 2
GERMANY

Bundesanstalt fur Geowissenschaften
und Rohstoffe
Attn: Michael Langer
Postfach 510 153
3000 Hanover 51
GERMANY

Hahn-Meitner-Institut fur Kernforschung
Attn: Werner Lutze
Glienicker Strasse 100
100 Berlin 39
GERMANY

Institut fur Tieflagerung (4)
Attn: K. Kuhn
Theodor-Heuss-Strasse 4
D-3300 Braunschweig
GERMANY

Kernforschung Karlsruhe
Attn: K. D. Closs
Postfach 3640
7500 Karlsruhe
GERMANY

Physikalisch-Technische Bundesanstalt
Attn: Peter Brenneke
Postfach 3345
D-3300 Braunschweig
GERMANY

D. R. Knowles
British Nuclear Fuels, plc
Risley, Warrington, Cheshire WA3 6AS
1002607 GREAT BRITAIN

Shingo Tashiro
Japan Atomic Energy Research Institute
Tokai-Mura, Ibaraki-Ken
319-11 JAPAN

Netherlands Energy Research Foundation
ECN (2)
Attn: Tuen Deboer
L. H. Vons
J. Prij
Westerduinweg
P.O. Box 1
1755 ZG Petten, THE NETHERLANDS

Svensk Karnbransleforsorjning AB
Attn: Fred Karlsson
Project KBS
Karnbranslesakerhet
Box 5864
10248 Stockholm, SWEDEN

Sandia Internal

1510 J.C. Cummings
1514 J.G. Arguello
1514 H.S. Morgan
1550 C.W. Peterson
3141 S.A. Landenberger (5)
3145 Document Control (8) for DOE/OSTI
3151 G.C. Claycomb (3)
6000 D.L. Hartley
6232 W.R. Wawersik
6233 J.L. Krumhansl
6300 T.O. Hunter
6310 T.E. Blejwas, Acting
6313 L.E. Shephard
6315 M.D. Siegel
6340 W.D. Weart
6340 S.Y. Pickering
6341 R.C. Lincoln
6341 Staff (9)
6341 Sandia WIPP Central Files (10)
6342 D.R. Anderson
6342 Staff (11)
6343 T.M. Schultheis
6343 Staff (2)
6344 E. Gorham

6344 Staff (10)
6345 B.M. Butcher, Acting
6345 Staff (9)
6346 J.R. Tillerson
6346 Staff (7)
6621 J.C. Stormont (15)
6621 L.D. Tyler
8523 R.C. Christman (SNLL Library)
9300 J.E. Powell
9310 J.D. Plimpton
9320 M.J. Navratil
9325 L.J. Keck (2)
9330 J.D. Kennedy
9333 O. Burchett
9333 J.W. Mercer
9334 P.D. Seward

U S GOVERNMENT PRINTING OFFICE 1991—673-122-60003

END

DATE FILMED

01/03/92